Comptes Rendus

Géoscience

Sciences de la Planète

Tarik Kernif, Thierry Nalpas, Pierre Gautier, Sylvie Bourquin, Marc Poujol and François Fournier

Formation and preservation of colluvial sedimentary breccias during early extension: processes and facies organization

Original Article — Stratigraphy, Sedimentology

Formation and preservation of colluvial sedimentary breccias during early extension: processes and facies organization

Tarik Kernif[®] [*, a], **Thierry Nalpas**[®] [a], **Pierre Gautier**[a], **Sylvie Bourquin**[®] [a], **Marc Poujol**[®] [a] **and François Fournier**[®] [b]

[a] Univ. Rennes, CNRS, Géosciences Rennes, UMR 6118, 35000 Rennes, France

[b] Aix-Marseille Université, CNRS, IRD, Cerege, Um 34, 3 Place Victor Hugo (Case 67), 13331 Marseille Cedex 03, France

E-mails: kernif.tarik@gmail.com (T. Kernif), thierry.nalpas@univ-rennes1.fr
(T. Nalpas), pierre.gautier@univ-rennes1.fr (P. Gautier),
sylvie.bourquin@univ-rennes1.fr (S. Bourquin), marc.poujol@univ-rennes1.fr
(M. Poujol), fournier@cerege.fr (F. Fournier)

Abstract. In this study, we focused on the formation and preservation processes of colluvial sedimentary breccias within an extensional context. The breccias studied in this work (from Crete and the Pyrenees) are characterized by poorly sorted polygenic deposits of highly angular carbonate clasts whose size ranges from pebbles to blocks measuring several millimeters to several meters. This study shows that the colluvial sedimentary breccias were formed during extensional tectonics and are spatially associated with large-throw normal fault. They are related to the creation of a substantial topography in the footwall of the normal fault followed by its collapse on the hanging wall, leading to fast sediment accumulation and preservation. These breccias are organized, with pebble- to cobble-sized clasts near the slope of the fault while the mega-clasts, such as boulders and blocks, are preserved away from the slope. Such a clast size organization is indicative of a dry rockfall process and is opposite to that of alluvial fan systems dominated by gravity process involving water. This study also revealed that the breccias from the NE of the Pyrenees, encountered on both flanks of the Bas Agly syncline and previously attributed to the Lower Cretaceous, are related to a first phase of extension during the Upper Jurassic.

Résumé. Dans cette étude, nous nous sommes intéressés aux processus de formation et de préservation des brèches sédimentaires colluviales dans un contexte d'extension. Les brèches étudiées dans ce travail (provenant de Crète et des Pyrénées) sont caractérisées par des dépôts polygéniques mal triés de clastes carbonatés très anguleux dont la taille varie de galets à blocs mesurant plusieurs millimètres à plusieurs mètres. Cette étude montre que les brèches sédimentaires colluviales formées au cours de la tectonique en extension sont spatialement associées à des failles normales majeures et sont organisées avec des clastes de la taille de petits cailloux à galets près de la pente de la faille et des méga-clastes, tels que des gros cailloux et des blocs, loin de la pente, contrairement à ce que l'on trouve dans les systèmes de cônes alluviaux. Cette étude révèle également que les brèches rencontrées sur les deux

---

[*] Corresponding author.

1. Introduction

Breccias are rocks that can form in any type of geodynamic context [e.g., Shukla and Sharma, 2018]. The objective of this work is to analyze the internal organization of sedimentary breccias, the sedimentary processes and the associated deformation in order to assess the geodynamic context that prevailed during their formation.

This study focuses on the formation processes of sedimentary breccias occurring as large masses (i.e., a thickness greater than ~50 m and a lateral extension of several kilometers) and their preservation by studying two case localities: the Pleistocene deposits along the southern coast of Crete (Greece) and the Late Jurassic deposits of the Bas Agly syncline in the northeastern Pyrenees (France). Given the relatively young age of the Cretan breccias, they present two main advantages: (i) the tectonic setting during their deposition is well constrained, corresponding to the development of a large normal fault zone and (ii) the deposits are well preserved and were not disturbed by later deformation. For the Pyrenean breccias, our interpretation will therefore partly rely on the comparison with the Cretan case. The Pyrenean sedimentary breccias of the Bas Agly syncline were deposited prior to the Upper Cretaceous to Tertiary Pyrenean compression. As a consequence, the Cretan and Pyrenean examples are complementary in order to clarify the depositional processes and the role of the extension for the preservation of this type of breccia.

Detailed sedimentological analyses (clast size, clast shape, clast provenance, nature of matrix, stratonomy, etc.) of the studied outcrops will be used to understand how the various breccia facies formed over time and to assess their spatial and temporal distributions. We will demonstrate that, based on the vertical and horizontal relationship between the various breccia facies, it is possible to determine the depositional processes and to reconstruct a depositional model, in relation with the early stage of formation of an extensive basin.

2. Geological setting

2.1. *The Quaternary example: Crete*

The lower part of the thrust pile of the Hellenides outcrops in western Crete (Figure 1) and consists of a thick sequence of metamorphic nappes overlain by remnants of non-metamorphic nappes [e.g., Bonneau, 1984]. The contacts between these two nappes appear either as one or several late-orogenic extensional detachments [Fassoulas et al., 1994, Jolivet et al., 1994, 1996, Kilias et al., 1994, Thomson et al., 1998, 1999, Rahl et al., 2005]. Peak pressure–temperature conditions in the metamorphic nappes reached 10 ± 2 kbar and 400 ± 50 °C [Theye et al., 1992]. Because of these relatively low-grade conditions, the recrystallization of rocks has been limited, thereby making it easier to identify the protoliths.

This study area is found at the foot of the Lefka Ori Mountains (Figure 1); within and around these mountains, the non-metamorphic nappes are represented by the Tripolitza nappe (TP), which consists of grey to black massive micritic to microsparitic limestones and dolomites [Seidel, 2003, Klein et al., 2013]. The TP nappe was deposited between the Late Triassic and the Eocene [e.g., Creutzburg and Seidel, 1975, Bonneau and Karakitsios, 1979, Zambetakis-Lekkas et al., 1998]. The lowermost part of the TP nappe is intensely fractured, probably due to the vicinity of the detachment fault(s) separating it from the metamorphic nappes.

The following metamorphic nappes have been distinguished, from base to top (Figure 1): (i) the Plattenkalk nappe (PK), which consists of Mesozoic to Eocene [e.g., Fytrolakis, 1972, Bonneau, 1973] or even Oligocene metacarbonates and metaflysch [Bizon and Thiebault, 1974], which are mostly composed of dolomitic, thick-bedded deposits in the lower part and platy limestones interlayered with chert beds in the upper part [e.g., Hall and Audley-Charles, 1983, Bonneau, 1984]; (ii) the Trypali nappe (TR) exhibits a lithological association similar to the PK but is made of older (early Mesozoic) sedimentary
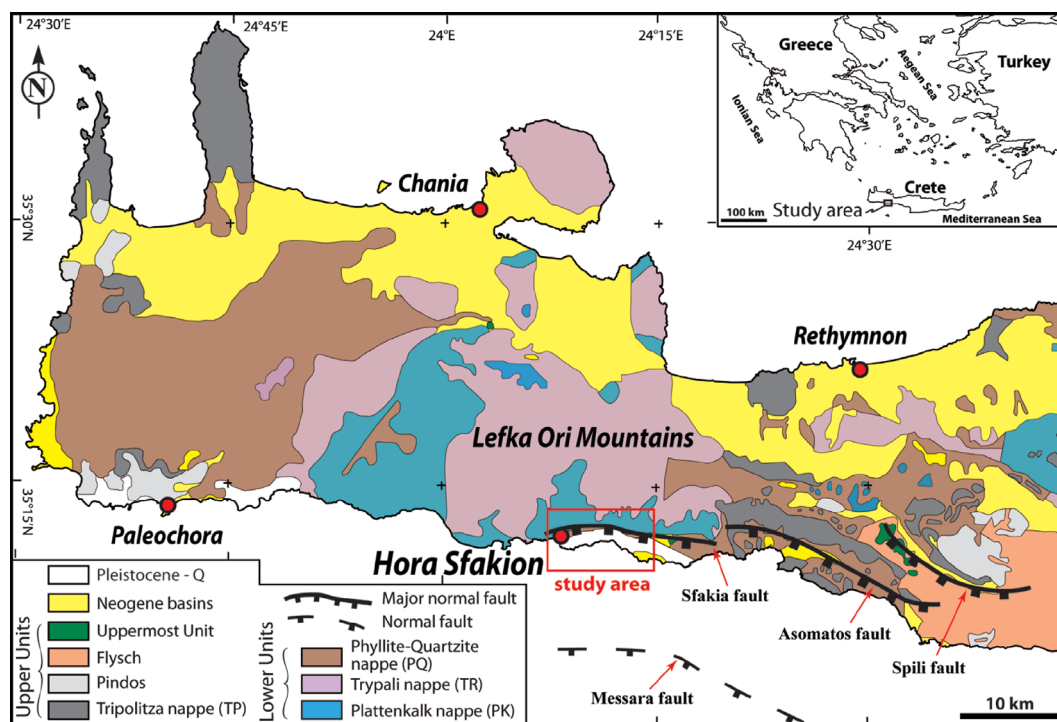
Figure 1. Simplified geological map of western Crete and location of the study area [modified after the IGME 1/200,000 geological map of Crete by Creutzburg et al., 1977; major normal fault taken from Caputo et al., 2010].

rocks including dolomites, pelmicritic limestones, detrital carbonates and breccias [Hall et al., 1984, Seidel, 2003, Rahl et al., 2004]; and (iii) the Phyllite–Quartzite nappe (PQ) consists of phyllites and lenticular quartzites with subordinate carbonates, evaporites and volcanic rocks [e.g., Greiling, 1982, Bonneau, 1984, Hall et al., 1984].

In southwestern Crete, the late Neogene N–S crustal extension led to the development of W–E to WNW–ESE striking and predominantly normal dip-slip faults [e.g., Angelier, 1979, Skourtsos et al., 2007, Caputo et al., 2010]. Three major south-dipping fault zones (70°–75° dip and scarp heights between 400 and 600 m), the Sfakia, Asomatos and Spili faults, are identified onshore while one major south-dipping fault zone (70° dip), the Messara fault, is localized off-shore [Caputo et al., 2010] (Figure 1). The study area is located along the Sfakia fault (SF), which forms a prominent topographic scarp separating the Lefka Ori Mountains from the Sfakion coastal piedmont (Figure 2). Thus, the Sfakia fault represents the major

fault limiting the uplift zone (Lefka Ori Mountains) and the subsidence zone (toward the Libyan Sea); this fault is therefore topographically similar to a borderline fault of an extensional basin. Extensional activity along the Sfakia fault was probably initiated during the early Pliocene, and significantly reduced during the late Pleistocene or the Holocene [Skourtsos et al., 2007, Tsimi et al., 2007]. Various large fan complexes formed by colluvial–alluvial deposits occur along the ~1.5 to 2.5 km wide coastal piedmont [Nemec and Postma, 1993, Vidakis et al., 1993, Pope et al., 2008]. To the west, five fans (Sfakia, Komitades, Vraskas, Nomikiana and Agios Nektarios) cover the whole piedmont (Figure 2). According to Pope et al. [2008, 2016], the fans started to develop during the late early Pleistocene. Nemec and Postma [1993] distinguished three main sedimentation stages during the development of the fans [see also Pope et al., 2008, 2016]: (i) during Stage 1, angular debris-flow deposits built small fans with depositional slopes of 20°–22°. The highly immature debris are viewed as
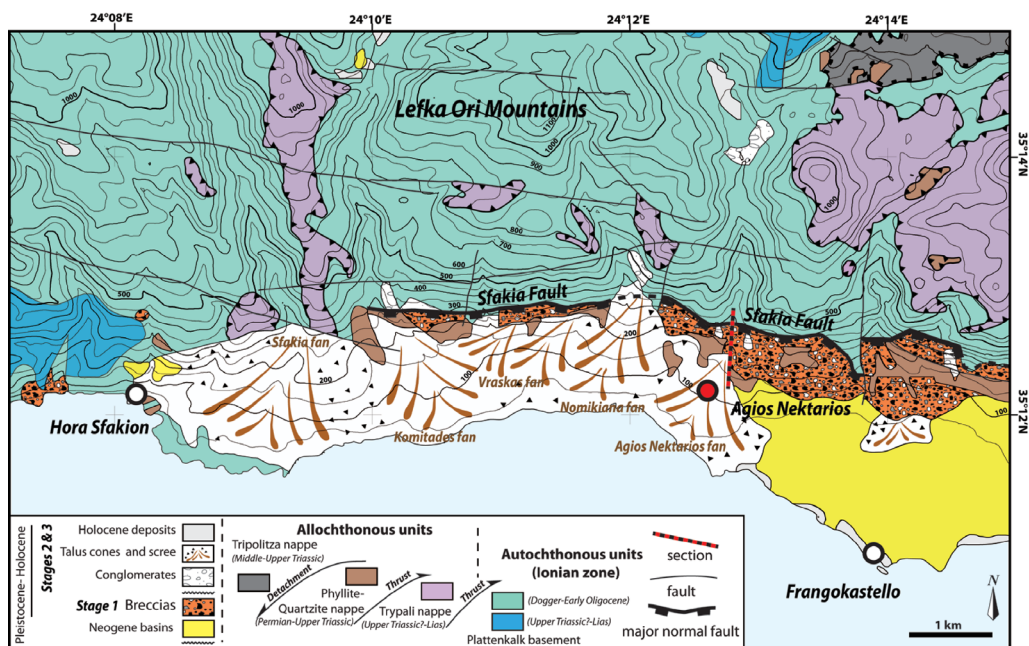
Figure 2. Geological map of the study area [modified after the IGME 1/50,000 geological map of Vrisses Sheet; Vidakis et al., 1993].

having derived locally through the headward erosion of mountain-front ravines; (ii) during Stage 2, streamflow deposits built a stack of large fan lobes which represent the bulk of the piedmont alluvium; (iii) Stage 3 is represented by minor Holocene unconsolidated gravel attributed to ephemeral streamflood surges.

The sedimentological and geochronological analyses undertaken by Nemec and Postma [1993] and Pope et al. [2016] were mostly derived from the study of the very large Sfakia Fan at the western end of the piedmont (Figure 2). Our study presents a revision of the Stage 1 depositional patterns as far east as the Agios Nektarios Fan.

2.2. *The ancient case study: Bas Agly*

The Bas Agly syncline is located in the easternmost area of the North Pyrenean Zone (NPZ, Figure 3). It is bounded to the southwest by the Agly Massif, to the north by the Saint Paul de Fenouillet syncline, and to the south and southeast by the Roussillon graben (Figure 3). The Upper Triassic of the Bas Agly syncline is composed of marine deposits with gypsum, marls

and dolomites and is characterized by a decollement level (gypsum). The evaporites allow for the decoupling between the Paleozoic (or Variscan) basement and the Mesozoic strata. The Upper Triassic to Lower Jurassic deposits often form a transgressive, infralittoral to circalittoral succession, dominated by alternating gray and red limestones and marls [e.g., Vaudin, 1982, Berger et al., 1993]. The Middle Jurassic to Lower Upper Jurassic deposits are mainly composed of massive black dolomites, alternating with calcareous dolomite and white limestones from inner carbonate platform environments [e.g., Berger et al., 1993].

The late Upper Jurassic-Early Cretaceous boundary is characterized by the presence of breccia deposits, named the "Brèche limite" in the region of Rivesaltes, Saint-Paul de Fenouillet, Tuchan and Leucate [e.g., Souquet and Debroas, 1980, Vaudin, 1982, Peybernès, 1976, Berger et al., 1993, Chelalou, 2015]. The studied "Brèche limite" outcrop is located on the northern and southern Bas Agly syncline flanks (Figure 3). This breccia is intercalated between lower Upper Jurassic and Berriasian limestone on both flanks of the Bas Agly syncline. Their process of forma-
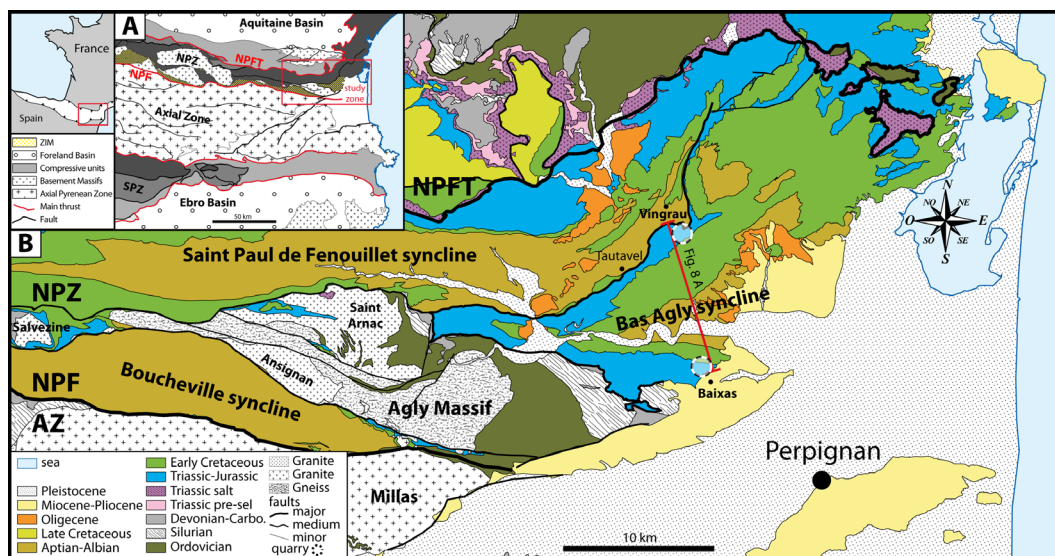
Figure 3. (A) Structural sketch map of the Pyrenean range simplified after the BRGM 1/1000,000 geological maps [IMZ: Internal Metamorphic Zone and Peridotite from Clerc, 2012]. (B) Simplified geological map of the study area modified after the BRGM 1/50,000 geological maps of Tuchan [Berger et al., 1997]; Perpignan [Berger et al., 1988]; Leucate [Bles and Berger, 1982]; Quillan [Crochet et al., 1989] and Rivesaltes [Fonteilles et al., 1993].

tion is attributed to result from large-scale tectonic instability of the region [e.g., Peybernès, 1976] and syntectonic deposition at the foot of major accidents [e.g., Souquet and Debroas, 1980]. More recently, Chelalou [2015] suggested that their formation is related to a phase of tectonic destabilization of the Jurassic carbonate platform that allowed the formation of slopes favoring gravity-driven processes leading to the deposition of sedimentary breccia, such an interpretation remaining hypothetical until today.

The "Brèche limite" is commonly confused with the so-called "Brèches post-albiennes" or "eocene breccia ebr," which are located at the Late Jurassic-Early Cretaceous boundary in the southern Bas Agly syncline flank and attributed to the Eocene (Bartonian) [e.g., Mattauer and Proust, 1962, Berger et al., 1993, Chelalou, 2015]. Our study focuses only on the formation and the preservation of the "Brèche limite" deposits intercalated between Upper Jurassic and Berriasian limestone.

A rifting phase at the end of the Jurassic is widely recorded in the North Atlantic Ocean as well as in northern Iberia and marks the beginning of the Early Cretaceous extension between the Iberian Penin-

sula and Europe [Péron-Pinvidic et al., 2007, Jammes et al., 2009]. In the studied quarries, breccias are overlain by Berriasian limestone [e.g., Berger et al., 1993] and Valanginian to early Aptian Urgonian limestone facies [e.g., Vaudin, 1982, Berger et al., 1993]. The Urgonian facies is composed of white limestones with rudists (bivalves) associated with *Orbitolina* (benthic foraminifera) characteristic of shallow-water carbonate platforms [e.g., Vaudin, 1982, Berger et al., 1993]. The opening of the Bay of Biscay, and the associated extension, resulted in the opening and filling of the basins (Saint Paul de Fenouillet, Boucheville and Bas Agly synclines) by a thick series of black marls (black flyschs) during the Aptian–Albian, which corresponds to the last series of the Mesozoic outcropping in the core of the Bas-Agly syncline [Debroas, 1987, 1990, Berger et al., 1993]. Lithospheric thinning has been shown to induce a high temperature–low pressure (HT/LP) metamorphism in the extensional basins of the NPZ [e.g., Choukroune and Mattauer, 1978, Golberg and Leyreloup, 1990, Clerc, 2012, Clerc et al., 2015, Chelalou, 2015, Chelalou et al., 2016, Ducoux, 2017, Odlum and Stockli, 2019]. At the end of the Santonian stage (~84 Ma), the initiation of the

convergence between the Iberian Peninsula and Europe led to the structural inversion of the Albo-Aptian basins, the reactivation of normal faults into thrust faults, the verticalization of folds limbs and finally the formation of the Pyrenees [e.g., Choukroune, 1976, Bessière et al., 1989, Sibuet et al., 2004, Ford and Vergés, 2020, Ducoux et al., 2021, Calvet et al., 2021].

3. Methodological approach

The two areas were investigated by means of a sedimentological analysis with field and thin section observations, facies description, spatial organization and temporal evolution [see Flügel, 2010]. In addition, the classification of Blair and McPherson [1999] was used to determine the clast sizes and grain sizes in order to create the abbreviations (code) used for the facies mentioned in this study.

Three sedimentological sections were compiled (≈1200 m in total): one in Crete, near the Agios Nektarios valley (Figure 2), and two on the southern and northern flanks of the Bas Agly syncline, in the northeastern Pyrenees (Figure 3). One hundred and fifty-two rock samples were collected along these three sections in order to prepare laboratory polished surfaces and thin sections, with the aim of describing the sedimentary characteristics of the various breccia facies.

The sedimentological characteristics observed in the field (Crete and Pyrenees) are clarified by standard petrographic analysis performed on the samples in the laboratory. Ten microbreccia facies samples were soaked in distilled water for 24 h and then passed through a 63 μ sieve. The microclasts trapped in the sieve were then dried and observed under a binocular microscope to visualize their roundness and sphericity.

4. Results: facies analyses and depositional model

4.1. *Facies analyses*

The sedimentary description of the Crete and Bas Agly sections have highlighted a total of six facies, detailed in Table 1 and pictured in Figure 4, ranging from massive breccia to stratified breccia. In sedimentary breccias, limestone or dolomitic clasts [e.g., Flügel, 2010] are very angular to sub-angular, with

sizes ranging from granules to blocks, that is, 4 mm to 65.5 m. The interclastic space (matrix) can be either a micrite, granule-sized clast, calcisiltite, calcarenite, or/and chemical precipitate (cement).

The facies descriptions presented in Table 1 can be used to suggest that both the clast size and the proportion of matrix are key parameters to identify the depositional processes. In order to identify the various facies, we propose a facies code that is largely based on the conglomerate classification of Blair and McPherson [1999]. The grain size classes used in this study can be subdivided as follows: (i) micro-breccias: granule (<2 to 4 mm); (ii) breccias: pebble (>4 to 64 mm) and cobble (>64 mm to 0.25 m); and (iii) mega-breccias: boulder (>0.25 m to 4.1 m), block (>4.1 m to 65.5 m) and slab (>65.5 m to 1 km, i.e., mega-breccias or internal gliding in this study). The following abbreviations are used in this study: breccias are indicated by a capital letter B, followed by 1 or 2 lowercase letter(s) to specify the size of the most prominent clasts (p: pebble, c: cobble, b: boulder), while, if present, the last letter (m) indicates the presence of a matrix.

4.1.1. *Agios Nektarios section (Crete)*

Description. The sedimentological section of the study area of Agios Nektarios valley in Crete shows, from base to top: (i) three distinct lithological units of breccias (denoted as I to III, Figure 5); these breccias consist mainly of matrix-supported breccias with unsorted clasts of variable sizes ranging from granules to blocks, the shape of the clasts is predominantly angular with low sphericity and (ii) one lithological unit of conglomerate (denoted as IV, Figure 5):

• **Unit I** is represented by the Bpm facies, formed by stratified microbreccia with large volume of micritic matrix (>80%), monogenic black dolomitic clasts (micrometric to granule-sized clasts, observed under an optical and binocular microscope) showing angular to sub-angular roundness and low sphericity. The presence of these clasts is characteristic of the Tripolitza nappe. The matrix of these breccias is composed of dolomicrite and/or calcisiltite.

• **Unit II** is represented by two facies, Bpcm and Bpbm, characterized by massive clasts or/and matrix-supported breccias and polygenic clasts within the breccias, coarsening upward. The internal beddings are indicated by vertical variations in the
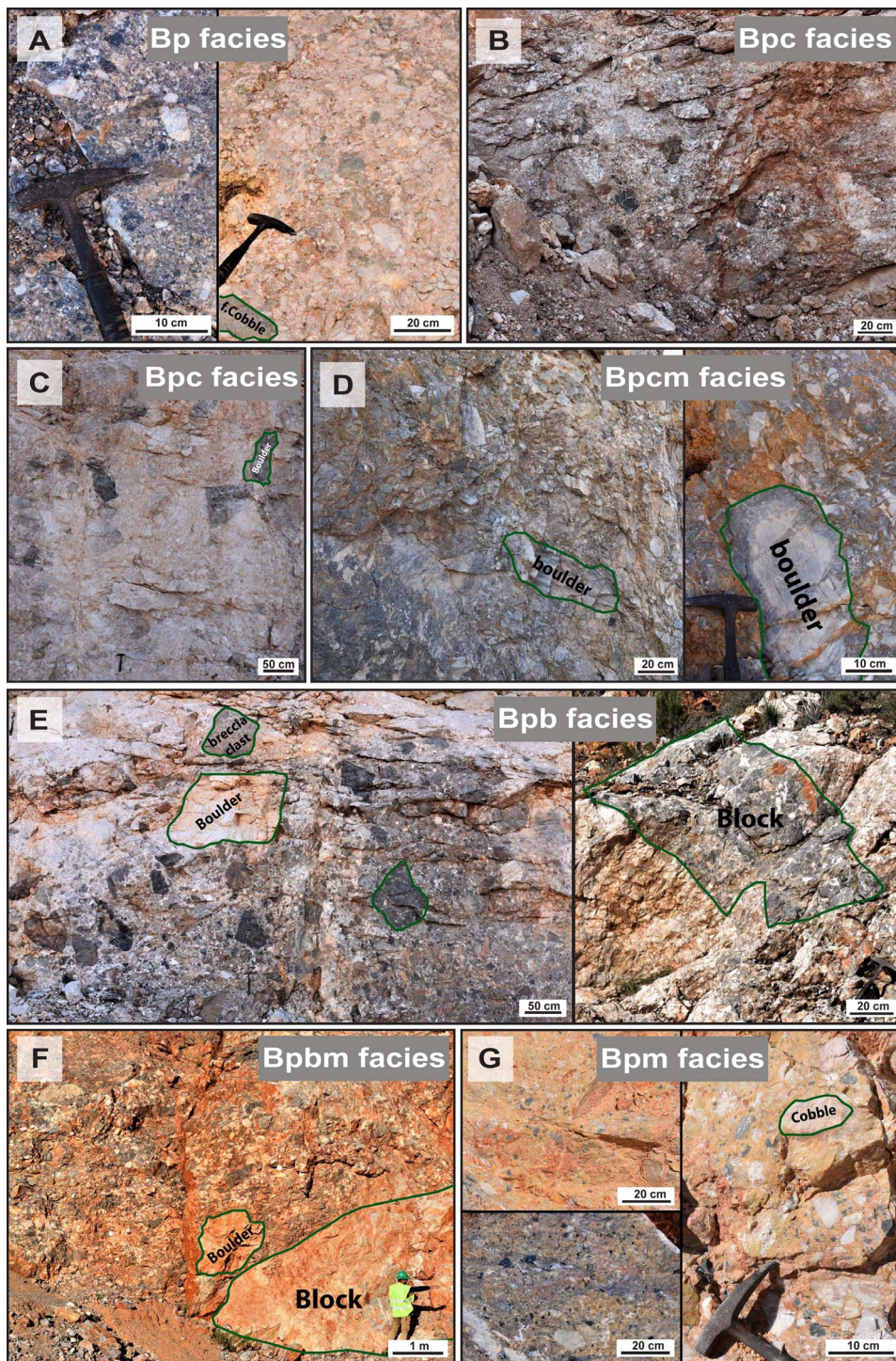
Figure 4. Caption continued on next page.

Figure 4 (cont.). Outcrop images of the different types of sedimentary breccia facies: (A) Bp facies, pseudo-monogenic breccias with very angular pebble-sized clasts and rarely angular fine cobble-sized clasts, (B) Bpc facies, polygenic breccias with very angular to angular coarse pebble- to fine cobble-sized clasts, (C) Bpc facies, pseudo-monogenic very angular to angular coarse pebble- to fine cobble breccias and showing the occasional presence of fine to medium boulder-sized clasts. (D) Bpcm facies, polygenic breccias with very angular to angular coarse pebble- to fine cobble-sized clasts and which can contain fine boulder-sized clasts, (E) Bpb facies, polygenic breccias with very angular to sub-angular coarse pebble- to coarse boulder-sized clasts and occasionally fine blocks, (F) Bpbm facies, polygenic breccias with very angular to sub-angular pebble- to very coarse boulder-sized clasts and coarse blocks, (G) Bpm facies, polygenic breccias with angular to sub-angular pebble-sized clasts and rarely sub-rounded fine cobble-sized clasts.

nature of clasts and/or matrix, forming steeply dipping (50° to 60° related to the tilting of layers during the extension), poorly stratified bodies. Clasts consist of fine pebbles to coarse boulders (from 4 mm to 4.1 m). The boulder-sized carbonate clasts show an organization in the direction of the falling rocks increasing size of the clasts downslope. The clasts are mainly very angular and with low sphericity except for the boulders which exhibit moderate to high sphericity. A detailed microscopic analysis shows that the clasts from these two facies (Bpcm and Bpbm) consist essentially of limestone and biomicritic and/or biosparitic dolomite. The matrix of these breccia facies is composed of microclasts ranging from granules to calcisiltites and/or calcisiltites to calcimicrites. However, in the top of this unit, there is a change in the nature of the clast sources since the black dolomitic clasts, characteristic of the Tripolitza nappe, are progressively replaced by metacarbonate clasts, rare quartzite clasts, highly altered phyllites from the Phyllite–Quartzites metamorphic nappe and clasts resulting from the reworking of the Unit I breccia.

- **Unit III** is characterized by a Bpbm facies, and the breccias are essentially composed of clasts from the Phyllite–Quartzite metamorphic nappe and rare various carbonate clasts. The clasts are essentially poorly sorted but the vertical succession displays an overall coarsening upward trend, with the clast size ranging from coarse pebbles to coarse boulders, i.e., 16 mm to 4.1 m. Occasional fine- to medium-sized blocks, from 4.1 to 16.4 m, can be observed at the top of this section (Figure 5). Like in the previous unit, this unit shows indistinct layers but with a decrease in the dip toward the top (30°). Petrographic analyses of thin sections show that the phyllites are very altered

and form the finest fraction of the matrix. Moreover, the matrix shows a granule-sized carbonate and/or calcarenitic fraction formed by micro-fragments and large mineral debris. At the top of this unit, associated with fine- to medium-sized phyllite blocks, i.e., 4.1 to 16.4 m, large volumes of limestone (pebble to cobble, i.e., 4 to 128 mm) have been observed, showing a peloidal mudstone texture with detrital carbonate and rare siliceous debris, strongly recrystallized, making it difficult to identify the allochems. These limestone clasts come from the lower nappes (Trypali and Plattenkalk nappe, respectively) of the Crete bedrock.

Note that clasts distribution from Unit II and Unit III show pebble- to cobble-sized clasts near the fault scarp while the mega-clasts, such as boulders and blocks, at a greater distance.

- **Unit IV** unconformably overlaying the breccia described for the previous units (Units I, II and III) is characterized by conglomerates, with rounded pebble- to cobble-sized clasts (Figure 6B). In contrast to Units I to III, breccia from Unit IV are well-stratified and display very low dips (<5°).

Such a vertical evolution in internal organization of breccia units, with a transitional upward decrease in dip, as well as the superimposition of Unit IV conglomerates over Units I, II and III breccias, is visible along the Agios Nektarios valley (Figure 6).

- These three breccia units (Units I, II and III) observed in the Agios Nektarios area are in contact with the metacarbonates from the Plattenkalk Nappe along the Sfakia normal fault (Figures 1, 2 and 6), where a tectonic breccia (cataclasite) has been evidenced and shows a thickness varying from ten centimeters to two meters in some places, and
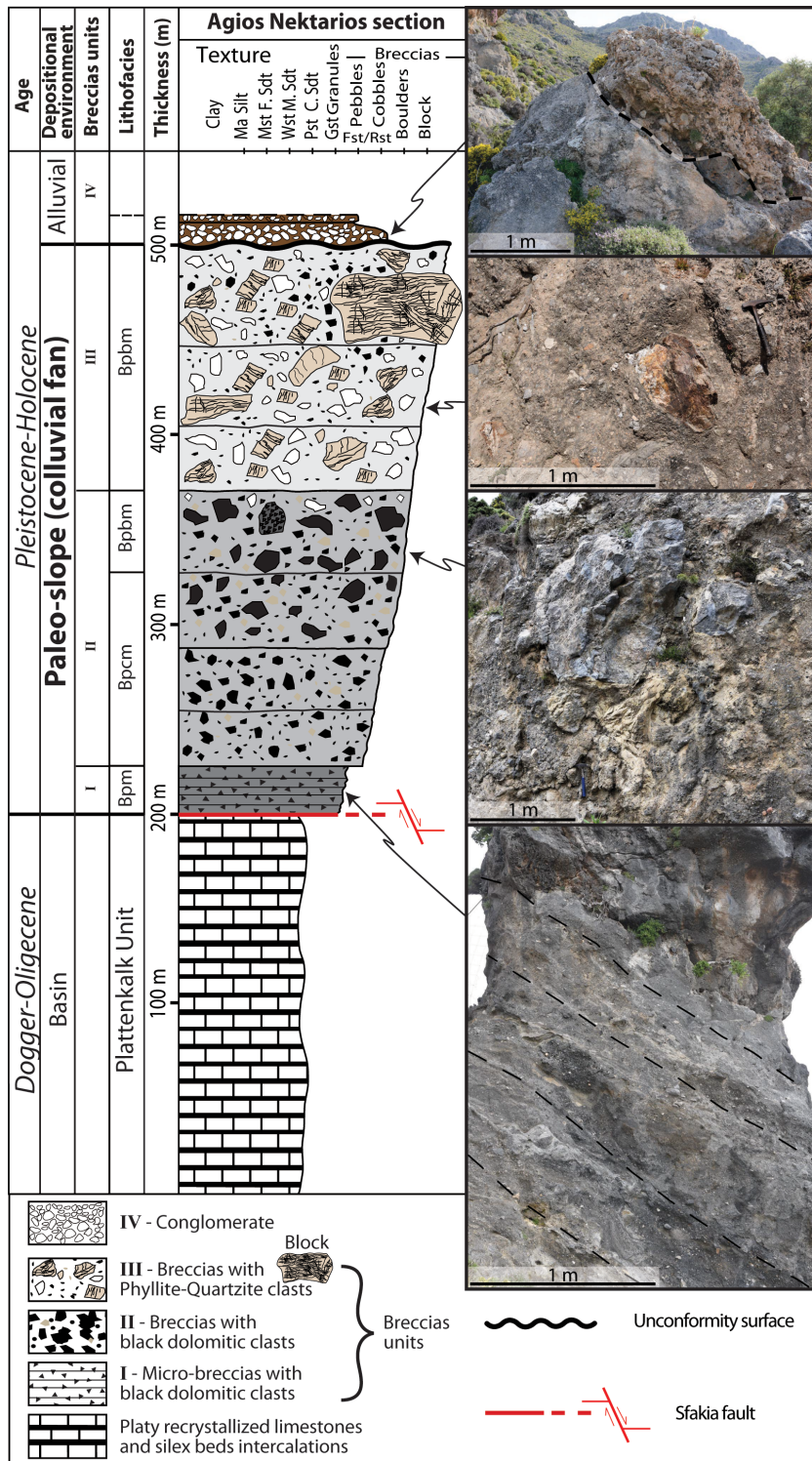
Figure 5. Sedimentological section of the study area (Agios Nektarios valley) located in southwestern Crete (see Figures 1 and 2 for location).

Table 1. Facies definition of the carbonate sedimentary breccia (Bas Agly syncline, Crete) and interpretations of the depositional processes

Facies code	Facies description	Interclastic space (matrix)	Depositional processes
Massive breccias			
Bp	Moderately sorted breccias with very angular pebble-sized clasts and rarely angular cobble-sized clasts, pseudo-monogenic, calcisiltite-matrix (Figure 4A)	<5%	
Bpc	Poorly sorted breccias with very angular to angular coarse pebble- to fine cobble-sized clasts and occasionally fine to medium boulder-sized clasts, pseudo-monogenic to polygenic, calcarenite-matrix and frequently meteoric cement phase (Figure 4B, C)	<10%	Rockfall generated by fault bedrock failure
Bpcm	Very poorly sorted breccias with very angular to angular coarse pebble- to fine cobble-sized clasts and which can contain fine boulder-sized clasts, polygenic, granule-sized clasts or/and micrite matrix-phase (Figure 4D)	<15%	
Massive mega-breccias			
Bpb	Unsorted breccias with very angular to sub-angular coarse pebble- to coarse boulder-sized clasts (occasionally fine blocks, polygenic, with an organization in the direction of the falling rocks increasing size of the clasts downslope), clast-supported, granule-sized clasts or calcarenite matrix (Figure 4E)	5–10%	Rockfall, rockslide generated by fault bedrock failure
Bpbm	Unsorted breccias with very angular to sub-angular pebble- to very coarse boulder-sized clasts, frequently blocks, polygenic, matrix supported, calcarenite or/and micrite rich-matrix (Figure 4F)	15–25%	
Stratified micro-breccias to breccias			
Bpm	Well-sorted stratified breccias with angular to sub-angular rich in granule-sized clasts, pebble-sized clasts and rarely sub-rounded fine cobble-sized clasts, monogenic to polygenic, muddy-matrix (Figure 4G)	>80%	Cohesive debris flows generated by intense rainfall

which varies in size from granule to clay as a result of intense grinding. The deformation affecting the breccias shows that in addition to the major fault (ESE–WNW, dip 70° south) that limits the metacarbonate bedrock of the breccias, various minor normal faults that are parallel to the major fault (Figure 6) also affect the whole breccias and are sealed by the conglomerate. These minor normal faults exhibit a metric to plurimetric vertical throw. Slip data collected on fault planes suggest an extension direction trending N–S to NNE–SSW along the Sfakia fault (Figure 6A) and NNE–SSW further east [Caputo et al., 2010]. In additional, the base of Unit I is affected by gently dipping (20°–30°) normal faults which likely represent gliding surfaces of unconsolidated (unlithified) breccia deposits, as evidenced by associated folds and slumps. These slumps are represented by a mixture of centimeter beds of granule to fine pebble-sized clasts with beds of dark-gray calcarenite and light-gray calcilutite.
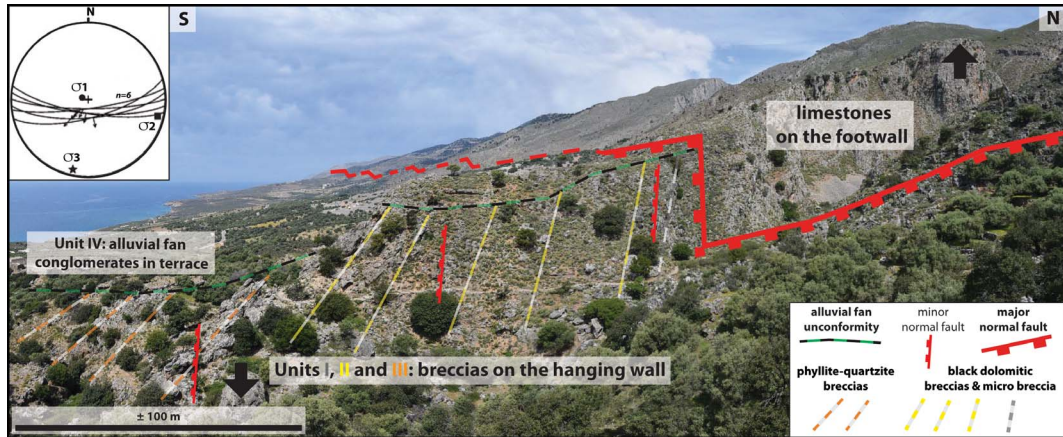
Figure 6. Panorama of the breccias in front of the Sfakia normal fault cut by the Agios Nektarios valley (in southwestern Crete). Top left corner frame shows stereographic projection of slip data collected by Caputo et al. [2010] on fault planes along the Sfakia fault.
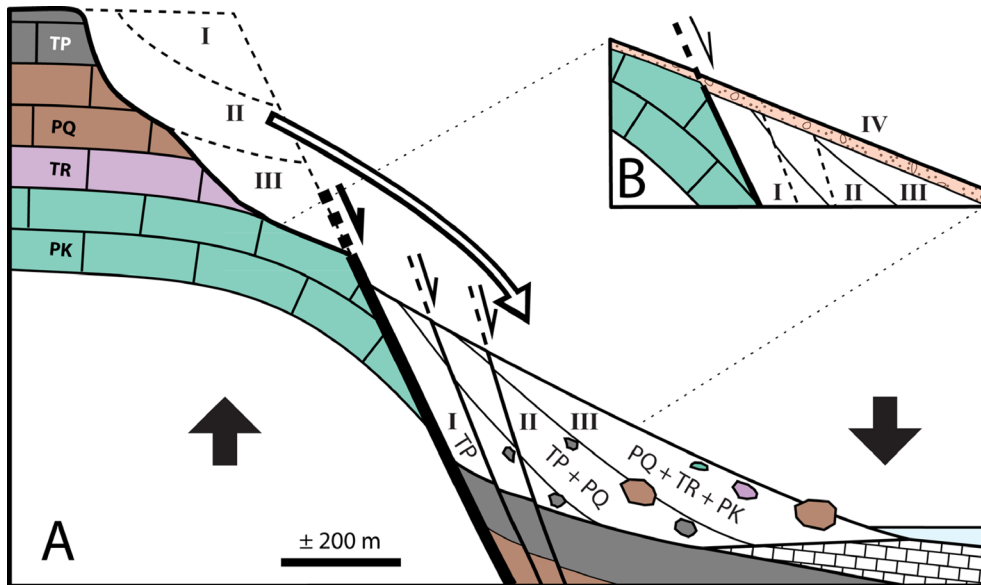
Figure 7. Breccia preservation model and the provenance of the clasts (Agios Nektarios valley, in southwestern Crete). The nappe codes are PK for Phyllite–Quartzite nappe, TR for Trypali nappe, PQ for Plattenkalk nappe, TP for Tripolitza nappe and for unit codes (I, II, III and IV) see Figures 1 and 5.

Interpretation. The Bpm facies observed in Unit I form a stratified unit and are characterized by angular to sub-angular clasts and a large volume of micritic matrix (80%), thus suggesting a deposition in the presence of a high proportion of water [e.g., Blair and McPherson, 1994a,b, Coussot and Meunier, 1996]. These criteria are typical of colluvial slope failures, with disintegration of a colluvial slide into a debris flow by entrainment of air and water through the jostling, deformation and loss of clast individuality as it moves downslope [Johnson and Rahn, 1970, Campbell, 1974, 1975, Costa, 1988]. This transformation requires the presence of water in the colluvium and is therefore most likely to occur during or immediately after excessive rainfall or snowmelt [Blair and McPherson, 1994a,b, Coussot and Meunier, 1996],

thus causing rapid infiltration and runoff to form a flash flood. As a consequence, this facies is attributed to a cohesive debris flow generated by intense rainfall (Table 1).

The Bpcm and Bpbm facies observed in Units II and III on the southwestern coast of Crete are characterized by angular to very angular carbonate clasts of various sizes, colors and origins. The interclastic space consists of rare sparry calcite cement, granule-sized clasts, calcisiltite, calcarenite and/or calcimicrite, which form massive units (indistinct layers). The unit exhibits an overall coarsening upward trend (pebbles to boulders and/or blocks) and pebble to cobble-sized clasts are located near the slope of the fault while the mega-clasts, such as boulders and blocks, are located far away from the slope (Figure 7). Deposits at the top of Units II and III partly derive from the reworking of the underlying breccias. Nemec and Postma [1993] have documented a preserved surficial depositional slope of 20°–22°. All of these criteria are indicative of a short transport, and these breccias likely result from the destabilization of a steep relief and are related to sedimentary processes that are active on colluvial fans at the base of a slope, formed by gravity flows [e.g., Church et al., 1979, Blair and McPherson, 1994a,b, 1995]. The increasing size of the clasts away from the fault (downslope) is due to fall sorting and the scarcity or a complete lack of muddy matrix during deposition, as larger clasts are heavier and therefore have greater kinetic energy [e.g., Rape, 1960, Gardner, 1979, Bones, 1973]. These processes result from rockfalls and rockslides generated by a fault bedrock failure in absence of water [e.g., Drew, 1873, Gardner, 1983, Sharpe, 1938, Mudge, 1965, Varnes, 1978, Blair and McPherson, 1994a, Table 1], where the biggest clasts acquire the greatest energy during their fall and therefore travel downslope farther than the smaller ones [e.g., Beaty, 1989, Beaty and DePolo, 1989, Gómez et al., 2003, De Blasio and Sæter, 2015]. This is marked not only by the upward coarsening trend of the units but also by an organization of the coarse boulder-sized clasts inside the layers of the units. These breccia deposits (or colluvium) are often misinterpreted and considered to represent a proximal part or an early stage of alluvial fan development [stage 1, see Blair and McPherson, 1994a]. The fall sorting of clasts in the colluvial fan is opposite to what is observed in an alluvial fan [e.g., Nemec and Steel, 1984, Nemec and

Postma, 1993, Blair and McPherson, 1994a,b, Leleu et al., 2009, Barrier et al., 2010] and is therefore a key parameter to discriminate breccias from these depositional environments.

Lastly, clast- to matrix-supported breccias from Unit IV with rounded Pebble- to cobble-sized clasts are interpreted as typical alluvial fan deposits in agreement with previous studies [Nemec and Postma, 1993, Pope et al., 2008].
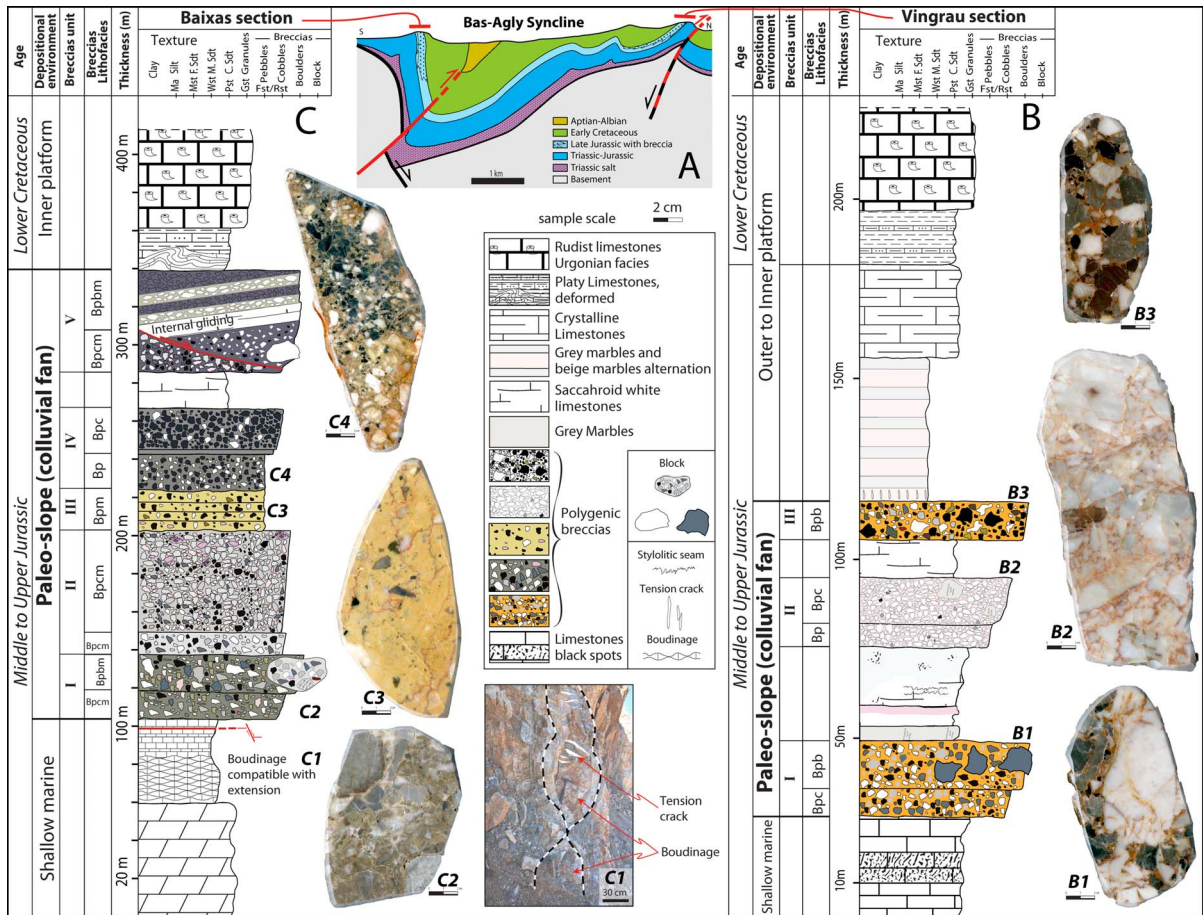
4.1.2. *Bas Agly syncline sections (Pyrenees)*

Description. The breccias from the Bas Agly Syncline crop out extensively in quarries and therefore detailed observations can be made. More specifically, the Vingrau section located in the eastern part of the Coume Roujou quarry (municipality of Vingrau), at the eastern extremity of the northern flank of the Bas Agly syncline, and the Baixas section located in the western part of the exploited Baixas quarry (municipality of Baixas), at the eastern extremity of the southern flank of the Bas Agly syncline (Figures 3 and 8A), have been studied in the present work. Three main facies groups have been identified from the two sedimentological sections analyzed from these quarries (Figure 8B, C). From base to top: (i) recrystallized mudstone and dolomites typical of the Bathonian to Oxfordian carbonate platform facies; (ii) a large mass of polygenic breccia (up to 250 m thick) with, locally, interbedded recrystallized mudstone to wackestone layers; and (iii) fissile recrystallized grainstone (~30 m thick), which form the Berriasian benchmark, overlain by white rudist-rich rudstones characterizing the lower Urgonian facies (i.e., Valanginian to early Aptian shallow-water carbonate platforms). In our study, we present the breccias (facies group ii) from both sections (Vingrau and Baixas):

Vingrau section (northern flank)

The Vingrau Breccias are composed of three units (denoted I to III, Figure 8B), which are stratigraphically above the Bathonian to Oxfordian limestones and below the Berriasian limestones. These units (I to III) are interbedded within recrystallized white limestone layers of initial mudstone to wackestone texture and are in stratigraphic contact with these different breccia units, which means that these limestones are interstratified within the breccias.

The breccia units (I to III) show a general chaotic character although an upward coarsening trend is

Figure 8. (A) Geological cross-sections through the eastern part of the North Pyrenean Zone (NPZ) illustrating the Bas Agly syncline and the location of the breccias studied in this work. (B) Sedimentological section of the Baixas quarry (Baixas, southern flank of the Bas Agly syncline). (C) Sedimentological section of the Coume Roujou quarry (Vingrau, northern flank of the Bas Agly syncline).

evidenced for the different units, ranging from a medium clast size (i.e., pebbles) to a very coarse clast size (i.e., cobbles, boulders or even blocks).

• **Unit I** overlies the Jurassic limestone bedrock and is represented by two facies (Bpc and Bpb), both consisting of a clast-supported accumulation of polygenic elements that show, in the thin sections, significant compaction features such as stylolitic seams around the clasts and concave–convex contacts. The breccias are made of angular carbonate clasts with low sphericity (except coarse boulder and block clasts showing a moderate to high sphericity). The interclast space consists of a matrix composed of calcisiltite- to calcarenite-sized clasts that are reddish-orange in color and occasionally

containing anisopachous calcite cement characterizing meteoric vadose environments. Polarized-light microscopic observations reveal that the matrix is frequently composed of mm-thick laminae displaying an upward coarsening trend, in which no fossils have been found. It is very difficult to discern individual layers within the breccia, but an upward coarsening trend from fine pebbles to coarse boulders has been evidenced from base to top within this unit.

• **Unit II** is dissimilar from the first unit and is represented by the Bp to Bpc facies with low matrix content (5 to 10%), showing a carbonate cemented breccia consisting essentially of white clasts with rare very angular grey clasts and large grey and/or black fine to medium boulders at the top that are
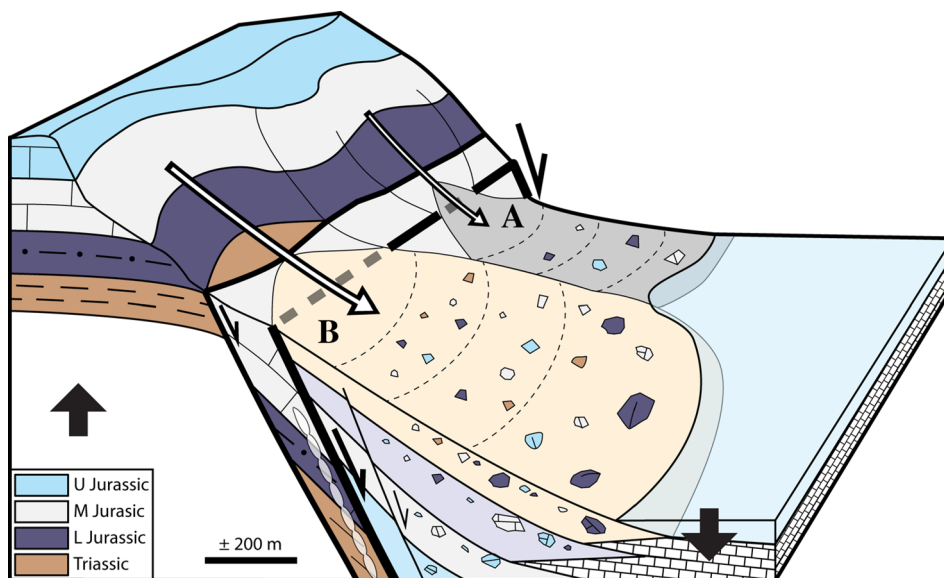
Figure 9. Breccia preservation model proposed for the Bas Agly Basin, Pyrenees (see Figure 3 for location). The small colluvial fan (A) resulting from extent of the destabilization area shows less variation with regard to clast lithology than colluvial fan (B) which resulted from a large destabilization area.

pseudo-monogenic in nature. The shape of the clasts is very angular with low to elongate sphericity. These breccias show moderately sorted clasts and an upward coarsening trend, which is not as apparent as in Unit I. The matrix consists of calcisiltite-sized clasts of reddish-pink color.

The clasts of Units I and II are previously described, derived from local rocks from the Mesozoic cover.

• **Unit III** is very similar to the upper part of Unit I (Bpb facies) but with a greater diversity of clast provenances. This unit is characterized by the presence of abundant black limestone clasts from the Lower Jurassic and by rarer Rhaetian yellow limestone clasts, with a very low matrix content. Although less abundant, the very coarse boulder-sized, carbonate clasts are still present in this unit, with subangular to sub-rounded shapes and high sphericity and are organized in the direction of the falling rocks increasing size of the clasts downslope.

The analysis of the thin sections shows that the breccias from Units I and II are essentially composed of limestone clasts with an initial mudstone to wackestone texture that has been partly recrystallized. These clasts contain poorly preserved biota, including foraminifera (essentially trocholines), echinoid fragments and bivalves. Also, in the Unit I, some clasts exhibit dedolomitization features. These facies characterize shallow and low energy environments specific to the Middle Jurassic and Lower Upper Jurassic inner platforms (Figure 9). We also find these clasts in the Unit III, but heavily enriched in foraminifera with uniserial forms (Lituolidae), dasycladacean green algae and gastropods. In addition, calcareous and marly bioclastic clasts of packstone texture that are very rich in ooids and bioclasts (echinoderms including ophiuroids and bivalves) characterize this Unit III. This faunal assemblage indicates an inflow of material coming mainly from the dismantling of the carbonate layers from outer environments (infralittoral to circalittoral) from the Upper Triassic to Lower Jurassic platforms (Figure 9).

Baixas section (southern flank)

In the Baixas breccias, five units have been identified (denoted I to V, Figure 8C), which are stratigraphically above the Bathonian to Oxfordian limestones and below the Berriasian limestones. The bedrock of these breccia units is made up of dolomites with a peloidal or pelletal packstone initial texture. Near the breccias, these limestones and dolomites exhibit boudinage features at different scales (Figure 8C1) in the vicinity of a fault zone at the base

of the breccias. The breccias result from a chaotic and poorly sorted polygenic accumulation of clasts, that is often matrix-supported and more rarely clast-supported. The calcareous clasts varying from very angular to sub-rounded in shape, with low to high sphericity, and are heterometric with their size ranging from pebbles to coarse blocks. The petrographic study shows that the interclastic space is filled with a dominantly micritic material, that is either associated with calcarenite, calcisiltite clasts and/or cement, or not. The matrix is devoid of microfossils.

Unit I is characterized by two polygenic breccia facies displaying upward coarsening trend (Figure 8C). The first, at the base, mainly consists of blue and grey, pebble- to cobble-sized clasts encased in a calcisiltite greenish matrix (Bpcm facies). The second facies, at the top, is characterized by pebble- to boulder-sized clasts with same color and calcarenitic greenish matrix (Bpbm facies). A plurimetric mega-block of polygenic breccia and bedrock clasts with a light grey matrix occurs at the top of the Bpbm breccia.

Breccias from **Unit II** exhibit a massive homogeneous Bpcm facies with a thickness of about 60 m (Figure 8C). This facies consists mainly of grey, black and pink, pebble- to cobble-sized clasts embedded within a micritic to calcisiltite light grey matrix at the base and calcarenitic dark grey matrix at the top.

Unit III is thinner than the other units, and is represented by the Bpm facies, which is made of stratified matrix-supported micro-breccias, with black and white granule- to pebble-sized clasts embedded in a yellow micritic matrix. Matrix represents more than 80% in volume of the whole breccia.

Unit IV is characterized by two polygenic clast-supported breccia facies (Bp and Bpc) displaying an upward coarsening trend (Figure 8C), exclusively formed by dark-blue and white clasts with a calcisiltite dark-grey matrix.

Unit V is composed of Bpcm and Bpbm breccia facies, together with interbedded meter-thick beds of monogenic breccias with white limestone clasts or recrystallized mudstone layer. Moreover, a white plurimetric mega-block (Figure 4F) occurs within a Bpbm breccia, showing a gliding plane that intersects the Bpcm facies (Figure 8C).

The analysis of the thin sections shows that the units from the Baixas breccias are composed with the same clasts and biological assemblage than the ones found in Units I and II from the Vingrau breccias.

The internal organization and sedimentological features of the Units I and IV are similar to those observed in Vingrau, particularly regarding the upward coarsening trend evidenced in Units I and III. Units I to IV from Baixas as well as the bedrock at the base and the Berriasian benchmark at the top of this unit show a dip toward the north, while breccias from Unit V display a dip toward the south–southwest. It should also be noted that the last two units (IV and V) are separated by a saccharoidal, recrystallized white limestone layers.

The contact between the limestone bedrock and the breccia is a north-verging steeply dipping normal fault (66N360). The faulted zone is composed of a 10 cm-thick cataclasite (core zone), and of a puzzle-shaped tectonic breccia (~1 m) above (damaged zone). Below this zone of fault deformation, boudinage features occur within the bedrock, which are consistent with a stretching parallel to the normal fault. Compared to the previous Vingrau section, minor normal faults that are generally dipping parallel to this fault are present in the Baixas quarry. Like in the Vingrau section, the Baixas breccias are capped by the same lower Cretaceous carbonate succession.

Interpretation. The breccias observed on the Bas Agly syncline of the Pyrenees present similar characteristics and processes than those observed on the southwestern coast of Crete. However, additional facies (Bp, Bpc, Bpb) are observed. The Bp and Bpc facies are interpreted as resulting from the same processes than those of the Bpcm facies and are attributed to rockfalls generated by fault bedrock failure [e.g., Drew, 1873, Gardner, 1983, Blair and McPherson, 1994a, Table 1]. The Bpb facies results from the same process as the Bpbm facies and is attributed to rockfall and rockslide processes generated during fault bedrock failure [e.g., Drew, 1873, Gardner, 1983, Sharpe, 1938, Mudge, 1965, Varnes, 1978, Blair and McPherson, 1994a, Table 1]. Therefore, the breccia deposits in the Bas Agly Basin result from gravity flow processes such as rockfalls and rockslides (Figure 9). The increasing size of the clasts downslope is due to fall sorting and to the scarcity of mud-matrix, as larger clasts are heavier and therefore have greater kinetic energy [e.g., Rape, 1960, Gardner, 1968, Bones, 1973]. In addition, the Late Jurassic period was subject to significant periods of extreme
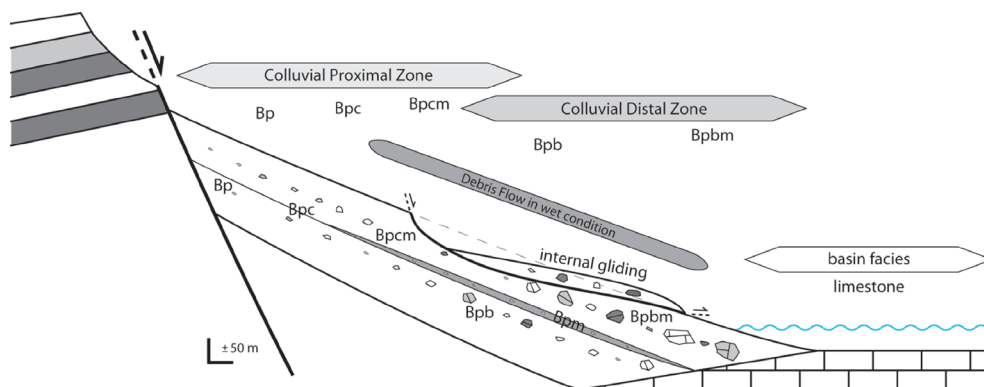
Figure 10. Depositional model for the breccia deposits during the first stage of the extensional basin, visualizing the different facies and facies associations of the sedimentary breccias and their organization from the proximal zone to the distal zone with regard to the fault.

dryness [e.g. Hesselbo et al., 2009, Dera et al., 2011, Martinez and Dera, 2015]. The scarcity of mud matrix is consistent with "dry" rockfalls in dry colluvial environment. In contrast, in alluvial fan deposits, debris flows are frequently characterized by a high matrix content so that coarse boulders or block can be transported over long distance within a matrix-supported flow [e.g., Harvey, 2012]. A lateral evolution between the breccia units in relation to the lithologic variation of the layers is affected by the destabilization of the hanging wall of the normal faults (Figure 9); as a result of this lithologic variation destabilized area, the colluvial cone deposits differ by the provenance of their clasts and can vary from monogenic to polygenic clasts (Figure 9A, B).

The main differences with the sedimentological sections studied in Crete are the presence of:

- breccia facies with very low matrix content (Bp, Bpc, Bpb facies);
- carbonate layers with a mudstone texture, interstratified within the breccias, mostly in the Vingrau section (Figure 8B); the short and curved micro-fractures filled with cement that characterize these limestones are typical of in situ destabilization whereas the sediment is still loose or very loosely consolidated. The presence of intercalated carbonate mudstones between the breccia intervals represents the subaqueous sedimentation of lime mud between two successive stages of relief destabilization and rockfall/rockslide breccia deposition.

4.2. *Facies association and depositional model of the colluvial fan during the initiation of the normal faults*

The facies detailed in Table 1 are positioned in the depositional model in Figure 10, ranging from pebble and cobble clast-sized near the normal fault in the Colluvial Proximal Zone (CPZ) to boulder and block clast-sized far from the normal fault in the Colluvial Distal Zone (CDZ), with occasional Debris Flow (DF) in wet conditions. These facies are grouped into three facies associations based on the fall sorting concept [e.g., Rape, 1960, Gardner, 1968, Bones, 1973] and are used to interpret depositional environments in this study (Table 2):

- Facies association CPZ is composed of three massive breccia facies, Bp, Bpc and Bpcm (Table 2), that are characterized by pebble- and cobble-sized clasts, as well as clast-supported and poor-matrix breccias related to the rockfall processes generated by a fault bedrock failure, representative of the proximal part of the subaerial colluvial fan deposit (Figure 10).

- Facies association CDZ is composed of two massive mega-breccias facies, Bpb and Bpbm (Table 2), essentially characterized by boulder and block-sized clasts, clast- to matrix-supported breccias related to rockfall and rockslides, such processes are representative of the distal part of the subaerial to subaqueous colluvial fan deposit (Figure 10). Internal gliding processes are generated by the increase of the layer dip associated to the progressive slip on

Table 2. Definition of the facies associations (Bas Agly syncline, Crete) and depositional environment interpretations

Name	Facie association	Depositional environment
CPZ	Massive breccias, pebble- to cobble-sized clast, clast-supported, and poor-matrix, represented by Bp, Bpc, Bpcm facies	Proximal zone of a subaerial colluvial fan deposit
CDZ	Massive mega-breccias, pebble- to block-sized clast, clast to matrix supported, represented by Bpb, Bpbm facies	Distal zone of a subaerial to subaqueous colluvial fan deposit
DF	Stratified micro-breccias to breccias, granule- to pebble-sized clasts, matrix-supported, represented by Bpm facies	Subaerial debris flows, which extends a large part of the slope

Abbreviations for the facies association: CPZ (Colluvial Proximal Zone); CDZ (Colluvial Distal Zone) and DF (Debris Flow). For the facies codes, see Table 1.

the fault, such processes are representative of the distal part of the subaerial to subaqueous colluvial fan deposit (Figure 10).

• Facies association DF, formed by the stratified micro-breccia facies Bpm (Table 2), is composed of granule to pebble-sized clasts, matrix-supported breccias related to subaerial cohesive debris flows, caused by colluvial slope gliding in response to the addition of a significant amount of water that underwent rapid infiltration and runoff to form a flash flood [e.g., Blair and McPherson, 1994a, Coussot and Meunier, 1996]. In this study, the DF facies association extends over a large part of the slope (Figure 10).

In both the Cretan and Bas Agly case studies, the breccias are deposited during the deformation and are associated with extensional tectonics, which provides the morphotectonic characteristics required to produce sedimentary breccia. The evolution of the depositional environments for the two stratigraphic columns investigated in the Bas Agly syncline show that the most proximal breccias are preserved in the Baixas zone whereas the most distal breccias are preserved in the Vingrau zone (Figure 8B, C). More distal breccia (Vingrau zone) are preserved in areas where limestone is also preserved (Figure 8B). In the case of Agios Nektarios valley in Crete, the breccias observed in the column are progressively further away from the Sfakia normal fault and thus change from proximal to distal breccias.

Therefore, the three stratigraphic columns from Crete and the Bas Agly syncline can be positioned within a general depositional profile of rockfalls, and rockslides associated with the major border normal fault of an extensional basin (Figure 11).

The stratigraphic columns of Crete and the Bas Agly syncline are indicative of the same depositional processes and represent different zones of a depositional profile within an extensional basin. These three stratigraphic columns can be used to capture the whole system from the proximal to the distal zone.

5. Discussion

5.1. *Relationships between depositional process and tectonic deformation*

In the quaternary analogue (Crete), during deformation in an extensional regime, the hanging wall of the normal fault subsides while its footwall is uplifted, thereby favoring the progressive rise of the relief of the Crete bedrock nappe (PK, TP, PQ, TR). Over time, this substantial local relief becomes unstable and then collapses, producing major rockfalls and rockslides.

The sedimentological section (Figure 5) representing the area along the Agios Nektarios valley allows us to observe the evolution of the breccia facies (Table 2) from the proximal zone to the distal zone, away from the normal fault (Figures 7, 11). The distribution of these facies shows an upward vertical coarsening trend. In addition, Unit I is exclusively composed of black dolomite clasts coming from the Tripolitza

Figure 11. Sedimentological sections for southwestern Crete and the Bas Agly Basin positioned on an integrated model.

nappe, Unit II is dominated by black dolomite with microfacies clasts coming from the lower part of the Tripolitza nappe and Unit III is composed of metamorphic clasts coming from the Phyllite–Quartzite nappe, as well as carbonate clasts from the Trypali nappe and non-metamorphic clasts from the Plattenkalk bedrock (Figure 5). This succession in the breccia units is indicative of a gradual arrival of clasts coming from the progressively exhumed reliefs of the footwall, during the movement of the normal fault (Figure 7). The source of the debris flow material may be both from the footwall and also partially from proximal zone of fine clast-sized breccia deposits. The initial maximum dip of the deposits is around 35°. After the movement of the fault, the deposits show a dip around 50° to 60° close to the fault dip. The order of arrival of the different clasts

in the sedimentary basin is linked to the successive exhumation (uplift) of the different source units along a tectonic structure (in this study, a normal fault). This order can be predicted by the *unroofing sequence* concepts [Colombo, 1994] which are used to provide evidence of gradual basin deformation. In this study, the earlier deposits derived from the denudation of the footwall (PK, TR, PQ, TP, Figure 7) are represented by sedimentary breccias with very angular clasts showing an unroofing sequence with an inverted distribution of clast arrival (TP, PQ, TR, PK, Figure 7) with respect to the source [normal sequence, see Colombo, 1994]. This means that the rockfall and rockslide processes are active during the whole period of normal fault activity and that the sedimentation and preservation of the breccias are syntectonic (Figure 7). The rockfall and rockslide

breccias appear to be coeval (syn-kinematic) with the normal faulting and are related to this tectonic process.

In the Mesozoic case study (Bas Agly syncline), more specifically in the Baixas quarry, a fault separates the breccias from the Upper Jurassic carbonates, and the layers of carbonate stratigraphically situated just below this fault present a typical boudinage-type deformation consistent with an extensional regime (Figures 8C, 9) [e.g., Goscombe et al., 2004]. As a result, we interpret this fault as a paleo-normal fault. In the Pyrenees, after the Upper Jurassic to Lower Cretaceous extensional phase, the Late Upper Cretaceous and Tertiary are characterized by compression–transpression [e.g., Choukroune, 1976, Bessière et al., 1989, Sibuet et al., 2004, Ford and Vergés, 2020, Ducoux et al., 2021, Calvet et al., 2021]. Therefore, the earliest faults created during the extension are difficult to find in the field because most of these normal faults were subsequently reactivated as reverse faults (Figure 8A) during compression and basin inversion [e.g., Nalpas et al., 1995]. The zone of boudinage associated with the fault that we interpret here as a normal fault corresponds to an early extensional deformation zone of the basin margin. In such an extensional tectonic setting, major sediment-gravity flows formed and the resulting breccias accumulated in the hanging wall where shallow subaquous sediments are deposited as evidenced by the interstratified limestones (Figures 8B, 9).

As a consequence, the predominantly subaerial nature of the breccias suggests stages of instantaneous infill of the subaqueous coastal space during gravity flow events, while intercalated shallow subaqueous carbonates are indicative of transgressions resulting from basin subsidence and/or eustatic pulses. In addition, increased fault activity may have favored the triggering of gravity flows and subsequent breccia deposition whereas autochthonous carbonate sedimentation may have prevailed during periods of tectonic quiescence. Variations in the slope of the uplifted blocks through time is another possible factor favoring slope destabilization and sedimentary breccia deposition.

In addition, it is not rare to find a disorganized superposition of the units; this is directly related to the movement of the normal fault that gradually increases the dip of the breccia layers and the gliding of these layers on the slope (Figure 12). It is very important to take into account the gliding of the breccia layers in a colluvial system because this internal gliding [or colluvial slides; Blair and McPherson, 1994a,b] may disorganize the layering; in addition, it may create specific geometries such as onlap around blocks and may produce deformation within breccias layers which could be mistakenly interpreted as regional tectonic deformations. The internal gliding (Figure 12) consists of intact masses of destabilized pre-existing colluvium that move downslope along a decollement level [Varnes, 1978, Bovis, 1986, Cronin, 1992]. Colluvial slides or internal gliding are more often initiated by the addition of rainfall or snowmelt when the sediment is significantly saturated with water [Caine, 1980, Ellen and Fleming, 1987, Reneau. et al., 1990].

The origin of the breccias is still under debate for specific areas in the North Pyrenean Zone (NPZ, Figure 3), while most of the breccias are associated with the Lower Cretaceous (Aptian–Albian) episode of lithospheric extension [e.g., Choukroune, 1973, Clerc et al., 2012]. The present work has demonstrated that the sedimentary breccias encountered on both flanks of the Bas Agly syncline are sedimentary breccias and are related to the destabilization of the hanging wall of the normal faults created during the Upper Jurassic extension. In addition, the observations and results of this study have established that: (i) Bas Agly breccias result from similar sedimentary processes as for the Pleistocene breccia from the southwestern coast of Crete; (ii) the order of arrival of the clasts (unroofing sequence) in the sedimentary basin evidences the syn-kinematic nature of the Bas Agly breccias; and (iii) breccias from the lower units are affected by syn-depositional faults which are sealed by breccias from the upper units (Figure 9). In addition, these breccias are intercalated between the Callovo-Oxfordian and upper Berriasian limestones [e.g., Jaffrezo, 1980], thereby suggesting a Kimmeridgian to lower Berriasian age for the breccias. These Upper Jurassic-lowermost Cretaceous breccias are called "brèche limite" on most geological maps (Rivesaltes, Saint-Paul de Fenouillet) of the northeastern Pyrenees.

This Jurassic lithospheric brittle extension associated with a high-dipping normal fault and the creation of a topographic gradient is consistent with the geodynamic reconstruction described by
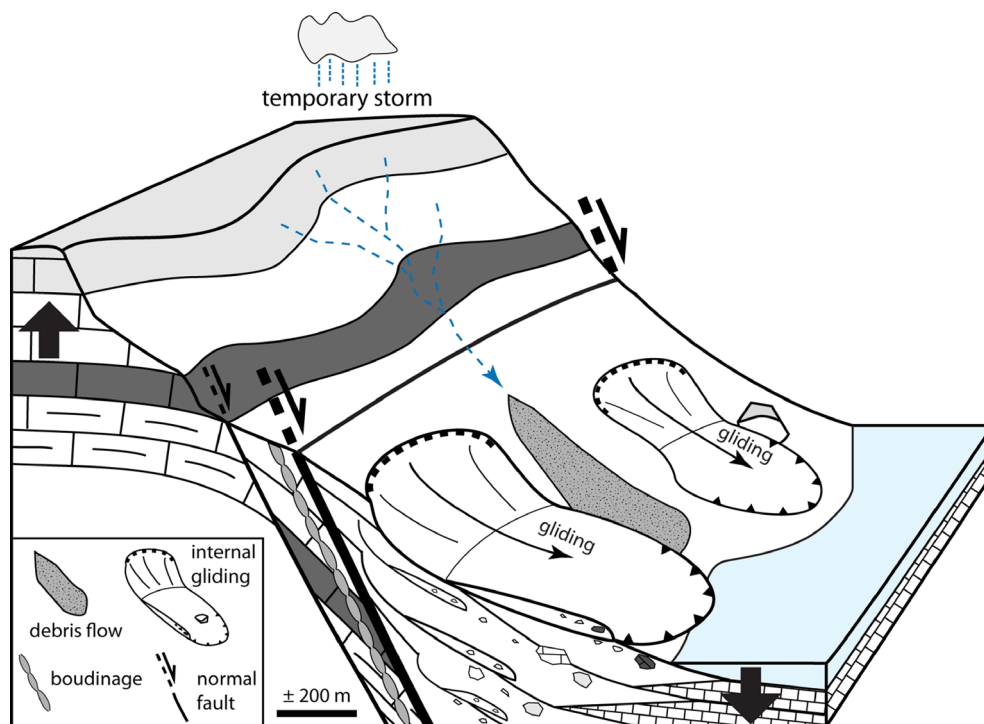
Figure 12. Schematic block diagram to visualize the internal gliding (colluvial slide) and debris flow process affecting the sedimentary breccias.

Péron-Pinvidic et al. [2007] and Jammes et al. [2009]. The structures created during this first Jurassic phase of extension serves as a guide for the Lower Cretaceous extension, which is described as being associated with high temperature and lithospheric boudinage and, as a result, with more ductile deformation at the scale of the lithosphere [e.g., Clerc et al., 2016, Lagabrielle et al., 2016].

This incipient Jurassic extension foreshadows the lower cretaceous extension in the whole Northern Pyrenean Zone. Some of the normal faults created during the Jurassic extension are certainly reactivated during the lower Cretaceous extension (Albo-Aptian times).

5.2. *Sedimentary breccia formation and preservation processes in extensional basins*

The breccias are deposited at the base of the slope created by the normal fault and therefore they fill the hanging wall, which represents a subsiding area. Subsidence of the hanging wall during the sedimentation of the breccia is a key parameter controlling their preservation and preventing the reworking of the clasts. In subsiding areas, the breccia deposits are rapidly covered by new layers of breccias and there is no time for the surface processes to smooth the edges of the clasts with water. This is not the case in talus-slope breccias where they are rarely preserved, since normal faults are absent [e.g., Sanders et al., 2009, Sanders, 2010].

Furthermore, in an extensive system, similar to a rift, the rivers flow in an opposite direction from the rift at the beginning of extension and the watersheds oriented toward the rift are very small or non-existent, in contrast to compressive systems where, in front of the main thrust, watersheds are very well developed. Recent studies on extensional basins have shown that positive precipitation–evaporation (P–E) balances prevail on the escarpment, while P–E deficits commonly occur on the rift floor [e.g., Bergner et al., 2009]. Therefore, along the rift borders, mass transfer is related to collapse processes such as rockfalls and rockslides and dominate toward the basin in the opposite direction to the main drainage (Figure 13).
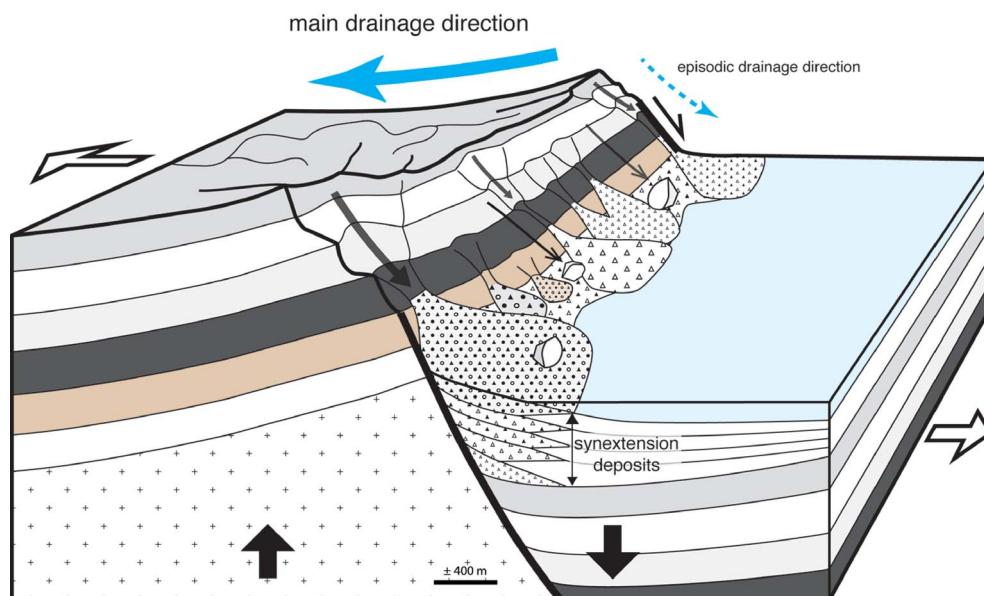
Figure 13. Schematic block diagram visualizing the formation and preservation of the sedimentary breccias during the early stage of the extensional basin.

These breccias are deposited at the beginning of the deformation in extension, and the parameters required to produce and preserved sedimentary breccias are met, i.e., (i) footwall uplift, which creates substantial topography, (ii) hanging wall rapid subsidence, (iii) the collapse of the topography, in the direction of the base of the slope of the normal fault, and (iv) rapid preservation to avoid the reworking of clasts by the drainage system. As a result, sedimentary breccias correspond to syn-tectonic deposits during the first stage of extensional basin formation that favors both the creation and preservation of sedimentary breccias. Sedimentary breccias may be considered as a typical lithology and a marker of continental extension.

After the deposition and preservation of the breccias, the surface of the slope created by the faults evolves and gradually decreases as the size of the watersheds oriented toward the rift increases. At one stage of the morphotectonic evolution of the extensional basin, the sedimentary flow coming from the watersheds oriented toward the rift becomes more substantial than the rockfall or rockslide and the breccias are reworked, eroded and replaced by conglomerates of alluvial fan systems, which unconformably overlie the breccias (e.g., Figures 5 and 7, denoted IV).

6. Conclusions

(1) Sedimentary breccias are deposited and preserved along major normal faults during extension and are related to the creation of substantial topography in the footwall and its collapse on the hanging wall with rapid preservation thereby preventing the reworking of the clasts.

(2) The sedimentary breccias studied here present common criteria, such as: (i) angulous to very angulous clasts of various sizes, (ii) of various origins, (iii) organized in massive units (indistinct layers) showing an upward coarsening, and (iv) the units of the breccias are organized with pebble- to cobble-sized clasts near the slope of the fault and the mega-clasts, such as boulders and blocks, far away from the slope. These features, as related to the movement of the normal fault and sedimentary processes active on the colluvial fans, favor rockfall, rockslide and internal gliding (colluvial slides) where clasts are supplied from the uplifted footwall of the fault and become coarser distally, in contrast with what is found in alluvial fan systems.

(3) A new terminology and nomenclature for the typical rockfall and rockslide processes of the sedimentary breccia facies has been proposed to serve as a reference in the future. We distinguish three facies associations: (i) the CPZ facies association, includes three massive breccia facies, Bp, Bpc and Bpcm, related to rockfall processes generated by fault bedrock failure, and is representative of the proximal part of the subaerial colluvial fan deposit, (ii) the CDZ facies association consists of massive megabreccias facies Bpb and Bpbm, related to the rockfall and rockslides generated by a fault bedrock failure, representative of the distal part of the subaerial to subaqueous colluvial fan deposit, (iii) the DF facies association consists of stratified micro-breccias to breccias related to subaerial cohesive debris flows.

(4) Sedimentary breccias associated with rockfall and rockslide processes correspond to syn-tectonic deposits during the early stage of the extensional basin formation and may be considered as a sedimentary marker of the initiation of continental extension.

(5) The breccias encountered on both flanks of the Bas Agly syncline, which are intercalated between Upper Jurassic and Berriasian limestone, are related to a first phase of extension during the Upper Jurassic and served as a guide for the Lower Cretaceous extension.

Conflicts of interest

Authors have no conflict of interest to declare.

Acknowledgements

References

Angelier, J. (1979). Determination of the mean principal directions of stresses for a given fault population. *Tectonophysics*, 56, TI7–T26.

Barrier, L., Proust, J. N., Nalpas, T., Robin, C., and Guillocheau, F. (2010). Control of alluvial sedimentation at foreland-basin active margins: a case study from the northeastern Ebro Basin (southeastern Pyrenees, Spain). *J. Sediment. Res.*, 80, 728–749.

Beaty, C. B. (1989). Great boulders I have known. *Geology*, 17, 349–352.

Beaty, C. B. and DePolo, C. M. (1989). Energetic earthquakes and boulders on alluvial fans: is there a connection? *Seismol. Soc. Am. Bull.*, 79, 219–224.

Berger, G. M., Bessière, G., Bilotte, M., and Viallard, P. (1997). *Carte géol. France (1/50 000), feuille Tuchan (1078)*. Bureau de recherches géologiques et minières (BRGM), Orléans.

Berger, G. M., Clauzon, G., Michaux, J., Suc, J.-P., Aloïsi, J.-C., Monaco, A., Got, H., Augris, C., Gadel, F., and Buscail, R. (1988). *Carte géol. France (1/50 000), feuille Perpignan (1091)*. Bureau de recherches géologiques et minière (BRGM), Orléans.

Berger, G. M., Fonteilles, M., Leblanc, D., Clauzon, G., Marshal, J. P., and Vautrelle, C. (1993). *Notice explicative, carte géol. France (1/50 000), feuille Rivesaltes (1090)*. BRGM, Orléans.

Bergner, A. G. N., Strecker, M. R., Trauth, M. H., Deino, A. L., Gasse, F., Blisniuk, P., and Dünforth, M. (2009). Tectonic and climatic control on evolution of rift lakes in the Central Kenya Rift, East Africa. *Quat. Sci. Rev.*, 28, 2804–2816.

Bessière, G., Bilotte, M., Crochet, B., Peybernès, B., Tambareau, Y., and Villate, J. (1989). *Notice explicative de la carte géologique de la France au 1/50.000, feuille de Quillan (1077)*. BRGM, Orléans.

Bizon, G. and Thiebault, F. (1974). Données nouvelles sur l'âge des marbres et quartzites du Taygète (Péloponnèse méridional, Grèce). *C. R. Acad. Sci. Paris*, 278, 9–12.

Blair, T. C. and McPherson, J. G. (1994a). Alluvial fan processes and forms. In Abrahams, A. D. and Parsons, A., editors, *Geomorphology of Desert Environments*, pages 354–402. Chapman & Hall, London.

Blair, T. C. and McPherson, J. G. (1994b). Alluvial fans and their natural distinction from rivers based on morphology, hydraulic processes, sedimentary processes, and facies. *J. Sed. Res.*, 64, 451–490.

Blair, T. C. and McPherson, J. G. (1995). Quaternary alluvial fans in southwestern Crete: sedimentation processes and geomorphic evolution, discussion. *Sedimentology*, 85, 531–535.

Blair, T. C. and McPherson, J. G. (1999). Grain-size and textural classification of coarse sedimentary particles. *J. Sediment. Res.*, 69, 6–19.

Bles, J. L. and Berger, G. M. (1982). *Carte géol. France (1/50 000), feuille Leucate (1079)*. Bureau de recherches géologiques et minières (BRGM), Orléans.

Bones, J. G. (1973). Process and sediment size arrangement on High Arctic Talus, Southwest Devon Island. N.W.T., Canada. *Arct. Alp. Res.*, 5(1), 29–40.

Bonneau, M. (1973). Ion affinities of epimetamorphic calcareous plates in Crete, carriage of Gavrovo Tripolitsa series and structure of aegean arc. *C. R. Acad. Sci.*, 277, 2453–2456.

Bonneau, M. (1984). Correlation of the Hellenide nappes in the south–east Aegean and their tectonic reconstruction. In Robertson, A. H. F. and Dixon, J. E., editors, *The Geological Evolution of the Eastern Mediterranean*, volume 17 of *Geological Society of London Special Publication*, pages 517–527. Blackwell, London.

Bonneau, M. and Karakitsios, V. (1979). Lower (Upper Triassic) Horizons of the Tripolitza Nappe in Crete (Greece) and their relationship with the phyllite nappe-problems of stratigraphy, tectonics and metamorphism. *C. R. Acad. Sci. Sér. D*, 28, 15–18.

Bovis, M. J. (1986). The morphology and mechanics of large-scale slope movement, with particular reference to southwest British Columbia. In Abrahams, A. D., editor, *Hillslope Processes*, pages 319–341. Allen & Unwin, Boston.

Caine, N. (1980). The rainfall intensity-duration control of shallow landslides and debris flows. *Geogr. Ann.*, 62A, 23–27.

Calvet, M., Gunnell, Y., and Laumonier, B. (2021). Denudation history and palaeogeography of the Pyrenees and their peripheral basins: an 84-million-year geomorphological perspective. *Earth-Sci. Rev.*, 215, article no. 103436.

Campbell, R. H. (1974). Debris flows originating from soil slips during rainstorms in southern California. *Q. J. Eng. Geol.*, 7, 339–349.

Campbell, R. H. (1975). *Soil Slips, Debris Flows, and Rainstorms in the Santa Monica Mountains and Vicinity, Southern California*, volume 851 of *Professional Paper*. United States Geological Survey.

Caputo, R., Catalano, S., Monaco, C., Romagnoli, G., Tortorici, G., and Tortorici, L. (2010). Active faulting on the island of Crete (Greece). *Geophys. J. Int.*, 183, 111–126.

Chelalou, R. (2015). *Formation et évolution du bassin de Boucheville, implication sur l'évolution tectonique, métamorphique et sédimentaire des bassins sédimentaires mésozoïques du Nord-Est des Pyrénées*. Thèse 3e cycle, Université Rennes 1. 181 p.

Chelalou, R., Nalpas, T., Bousquet, R., Prevost, M., Lahfid, A., Ringenbach, J. C., and Ballard, J. F. (2016). New sedimentological, structural and paleo-thermicity data on the Boucheville basin (eastern north Pyrenean zone, France). *C. R. Geosci.*, 348, 312–332.

Choukroune, P. (1973). La brèche de Lherz dite "d'explosion liée à la mise en place des lherzolites" est une brèche sédimentaire d'âge cénozoïque. *C. R. Acad. Sci.*, 277, 2621–2624.

Choukroune, P. (1976). Structure et évolution tectonique de la zone nord pyrénéenne. *Mem. Soc. Géol. Fr.*, 127, 1–116.

Choukroune, P. and Mattauer, M. (1978). Tectonique des plaques et Pyrenees : Sur le fonctionnement de la faille Nord-Pyrénéenne ; comparaison avec les modules actuels. *Bull. Soc. Géol. Fr.*, 20, 689–700.

Church, M., Stock, R. F., and Ryder, J. M. (1979). Contemporary sedimentary environments on Baffin Island, N.W.T., Canada: debris slope accumulations. *Arct. Alp. Res.*, 11, 371–402.

Clerc, C. (2012). *Evolution du domaine nord-pyrénéen au Crétacé. Amincissement crustal extrême et thermicité élevée : un analogue pour les marges passives*. Thèse 3e cycle, Université Pierre et Marie Curie — Paris VI.

Clerc, C., Lagabrielle, Y., Labaume, P., Ringenbach, J. C., Vauchez, A., and Nalpas, T. (2016). Basement-Cover decoupling and progressive exhumation

of metamorphic sediments at hot rifted margin. Insights from the Northeastern Pyrenean analog. *Tectonophysics*, 686, 82–97.

Clerc, C., Lagabrielle, Y., Neumaier, M., Reynaud, J. Y., and De Saint Blanquat, M. (2012). Exhumation of subcontinental mantle rocks: evidence from ultramafic-bearing clastic deposits nearby the Lherz peridotite body, French Pyrenees. *Bull. Soc. Géol. Fr.*, 183, 443–459.

Clerc, C., Lahfid, A., Monié, P., Lagabrielle, Y., Chopin, C., Poujol, M., Boulvais, P., Ringenbach, J. C., Masini, E., and De St Banquat, M. (2015). High-temperature metamorphism during extreme thinning of the continental crust: a reappraisal of the North Pyrenean passive paleomargin. *Solid Earth*, 6, 643–668.

Colombo, F. (1994). Normal and reverse unroofing sequences in syntectonic conglomerates as evidence of progressive basinward deformation. *Geology*, 22, 235–238.

Costa, J. E. (1988). Rhenlogic, geomorphic, and sedimentologic differentiation of water floods, hyperconcentrated flows, and debris flows. In Baker, V. R., Kochel, R. C., and Parian, P. C., editors, *Flood Geomorphology*, pages 113–122. Wiley, New York.

Coussot, P. and Meunier, M. (1996). Recognition, classification and mechanical description of debris flows. *Earth-Sci. Rev.*, 40, 209–227.

Creutzburg, N., Drooger, C. W., and Meulenkamp, J. E. (1977). *General Geologic Map of Crete 1:200.000*. Institute of Geological and Mining Research (IGME), Athens.

Creutzburg, N. and Seidel, E. (1975). Zum Stand der Geologie des Praneogens auf Kreta. *Jb. Geol. Palaontol. Abh.*, 149, 363–383.

Crochet, B., Villatte, J., Tambareau, Y., Bilotte, M., Bousquet, J.-P, Kuhfuss, A., Bouillin, J. P., Gelard, J.-P., Bessière, G., and Paris, J.-P. (1989). *Carte géol. France (1/50 000), feuille Quillan (1077)*. Bureau de recherches géologiques et minières (BRGM), Orléans.

Cronin, V. S. (1992). Compound landslides: nature and hazard potential of secondary landslides within host landslides. In Slossen, J. E., Keene, A. G., and Johnson, J. A., editors, *Landslides/Landslide Mitigation: Geological Society of America Reviews in Engineering Geology*, volume 9, pages 1–9. Geological Society of America, Boulder, CO.

De Blasio, F. V. and Sæter, M. B. (2015). Dynamics of grains falling on a sloping granular medium: application to the evolution of a talus. *Earth Surf. Process. Landf.*, 40(5), 599–609.

Debroas, E. J. (1987). Le flysch à fucoïdes d'Uchentein témoin d'un escarpement turono-sénonien inférieur de la paléofaille nord-pyrénéenne, Pyrénées centrales, France. Fucoidal Flysch Uchentein Indic. Turonian-Low. *Senonian Escarpm. Of.*, 3, 77–93.

Debroas, E. J. (1990). Le flysch noir albo-cenomanien temoin de la structuration albienne a senonienne de la Zone nord-pyreneenne en Bigorre (Hautes-Pyrenees, France). *Bull. Soc. Géol. Fr.*, 6, 273–285.

Dera, G., Brigaud, B., Monna, F., Laffont, R., Pucéat, E., Deconinck, J.-F., Pellenard, P., Joachimski, M., and Durlet, C. (2011). Climatic ups and downs in a disturbed Jurassic world. *Geology*, 39(3), 215–218.

Drew, F. (1873). Alluvial and lacustrine deposits and glacial records of the Upper Indus Basin. *Geol. Soc. Lond. Q. J.*, 29, 441–471.

Ducoux, M. (2017). *Structure, thermicité et évolution géodynamique de la Zone Interne Métamorphique des Pyrénées*. PhD thesis, University of Orléans, France. 646 p.

Ducoux, M., Jolivet, L., Cagnard, F., and Baudin, T. (2021). Basement-cover decoupling during the inversion of a hyperextended basin: Insights from the Eastern Pyrenees. *Tectonics*, 40, article no. e2020TC006512.

Ellen, S. D. and Fleming, R. W. (1987). Mobilization of debris flows from soil slips, San Francisco Bay region, California. In Costa, J. E. and Wieczorek, G. F., editors, *Debris Flows/Avalanches: Process, Recognition, and Mitigation: Geological Society of America Reviews in Engineering Geology*, volume 7, pages 31–40. Geological Society of America, Boulder, CO.

Fassoulas, C., Kilias, A., and Mountrakis, D. (1994). Postnappe stacking extension and exhumation of high-pressure low-temperature rocks in the Island of Crete, Greece. *Tectonics*, 13, 127–138.

Flügel, E. (2010). *Microfacies of Carbonate Rocks: Analysis, Interpretation and implications*. Springer-Verlag, Berlin, New York, 2nd edition.

Fonteilles, M., Leblanc, D., Clauzon, G., Vaudin, J. L., and Berger, G. M. (1993). *Carte géol. France (1/50 000), feuille Rivesaltes (1090)*. Bureau de recherches géologiques et minières (BRGM), Orléans.

Ford, M. and Vergés, J. (2020). Evolution of a salt-rich transtensional rifted margin, eastern North

Pyrénées, France. *J. Geol. Soc.*, 178(1), 2019–2157.

Fytrolakis, N. (1972). Die Einwirkungen gewisser orogener Bewegungen und die Gipsbildung in Ostkreta (Prov. Sitia). *Bull. Geol. Soc. Greece*, 9, 81–100.

Gardner, J. S. (1968). *Debris Slope Form and Processes in the Lake Louise District, A High Mountain Area*. PhD thesis, McGill University. 263 p. (Unpublished).

Gardner, J. S. (1979). The movement of material on debris slopes in the Canadian Rocky Mountains. *Z. Geomorphol.*, 23, 45–67.

Gardner, J. S. (1983). Accretion rates on some debris slopes in the ML Rae area, Canadian Rocky Mountains. *Earth Surface Process. Landf.*, 8, 347–355.

Golberg, J. M. and Leyreloup, A. F. (1990). High temperature–low pressure Cretaceous metamorphism related to crustal thinning (Eastern North Pyrenean Zone, France). *Contrib. Mineral. Petrol.*, 104, 194–207.

Gómez, A., Palacios, D., Luengo, E., Tanarro, L. M., Schulte, L., and Ramos, M. (2003). Talus instability in a recent deglaciation area and its relationship to buried ice and snow cover evolution (Picacho del Veleta, Sierra Nevada, Spain). *Geogr. Ann. A*, 85(2), 165–182.

Goscombe, B. D., Passchier, C. W., and Hand, M. (2004). Boudinage classification: end-member boudin types and modified boudin structures. *J. Struct. Geol.*, 26(4), 739–763.

Greiling, R. (1982). The metamorphic and structural evolution of the Phyllite-quartzite nappe of western Crete. *J. Struct. Geol.*, 4, 291–297.

Hall, R. and Audley-Charles, M. G. (1983). The structure and regional significance of the Talea–Ori. *Crete. J. Struct. Geol.*, 5, 167–179.

Hall, R., Audley-Charles, M. G., and Carter, D. J. (1984). The significance of Crete for the evolution of the Eastern Mediterranean. In Dixon, J. E. and Robertson, A. H. F., editors, *The Geological Evolution of the Eastern Mediterranean*, volume 17 of *Special Publication*, pages 499–516. Geological Society, London.

Harvey, A. M. (2012). The coupling status of alluvial fans and debris cones: A review and synthesis. *Earth Surf. Process. Landf.*, 37(1), 64–76.

Hesselbo, S. P., Deconinck, J.-F., Huggett, J. M., and Morgans-Bell, H. S. (2009). Late Jurassic palaeoclimatic change from clay mineralogy and gamma-ray spectrometry of the Kimmeridge Clay, Dorset.

UK *J. Geol. Soc. Lond.*, 166, 1123–1134.

Jaffrezo, M. (1980). *Les formations carbonatées des Corbières (France) du Dogger à l'Aptien : micropaléontologie stratigraphique, biozonation, paléoécologie. Extension des résultats à la Mésogée.* Thèse d'état, Université Paris VI. 615 p.

Jammes, S., Manatschal, G., Lavier, L., and Masini, E. (2009). Tectonosedimentary evolution related to extreme crustal thinning ahead of a propagating ocean: Example of the western Pyrenees. *Tectonics*, 28, article no. TC4012.

Johnson, A. M. and Rahn, P. H. (1970). Mobilization of debris flows. *Z. Geomorphol. Supplementband*, 9, 168–186.

Jolivet, L., Brun, J. P., Gautier, P., and Lallemant, S. (1994). 3-D kinematics of extension in the aegean from the early miocene to the present. *Bull. Soc. Géol. Fr.*, 165, 195–209.

Jolivet, L., Goffé, B., Monié, P., Truffert-Luxey, C., Patriat, M., and Bonneau, M. (1996). Miocene detachment in Crete and exhumation P-T-t paths of high-pressure metamorphic rocks. *Tectonics*, 15, 1129–1153.

Kilias, A., Fassoulas, C., and Mountrakis, D. (1994). Tertiary extension of continental crust and uplift of Psiloritis metamophic core complex in the central part of the Hellenic Arc (Crete, Greece). *Geol. Rundsch.*, 83, 417–430.

Klein, T., Craddock, J. P., and Zulauf, G. (2013). Constraints on the geodynamical evolution of Crete: insights from illite crystallinity, Raman spectroscopy and calcite twinning above and below the "Cretan Detachment". *Int. J. Earth Sci.*, 102, 139–182.

Lagabrielle, Y., Clerc, C., Vauchez, A., Lahfid, A., Labaume, P., Azambre, B., Fourcade, F., and Dautria, J.-M. (2016). Very high geothermal gradient during mantle exhumation recorded in mylonitic marbles and carbonate breccias from a Mesozoic Pyrenean paleomargin (Lherz area, North Pyrenean Zone, France). *C. R. Geosci.*, 348(3–4), 290–300. (Special Issue, The Pyrénées).

Leleu, S., Ghienne, I. F., and Manatschal, G. (2009). Alluvial fan development and morpho tectonic evolution in response to contractional fault reactivation (late cretaceous–paleocene), provence, France. *Basin Res.*, 21, 157–187.

Martinez, M. and Dera, G. (2015). Orbital pacing of carbon fluxes by a~9-My eccentricity cycleduring the Mesozoic. *Proc. Natl. Acad. Sci. USA*, 112,

12604–12609.

Mattauer, M. and Proust, F. (1962). Sur l'âge post-albien de quelques brèches réputées jurassiques ou néocomiennes des Pyrénées orientales. *C. R. Somm. Soc. Geol. Fr.*, 10, 304–305.

Mudge, M. R. (1965). Rockfall-avalanche and rockslide-avalanche deposits at Sawtooth Ridge, Montana. *Geol. Soc. Am. Bull.*, 76, 1003–1014.

Nalpas, T., Le Douaran, S., Brun, J. P., Unterneher, P., and Richert, J. P. (1995). Inversion of the Broad Fourteens Basin (offshore Netherlands), a small-scale model investigation. *Sediment. Geol.*, 95, 237–250.

Nemec, W. and Postma, G. (1993). Quaternary alluvial fans in southwestern Crete: sedimentation processes and geomorphic evolution. In Marzo, M. and Puigdefábregas, C., editors, *Alluvial Sedimentation*, volume 17 of *Special Publication*, pages 235–276. International Association of Sedimentologists.

Nemec, W. and Steel, R. J. (1984). Alluvial and coastal conglomerates: Their significant features and some comments on gravelly mass-flow deposits. In Koster, E. H. and Steel, R. J., editors, *Sedimentology of Gravels and Conglomerates*, volume 10 of *Memoir*, pages 1–31. Canadian Society of Petroleum Geologists.

Odlum, M. L. and Stockli, D. F. (2019). Thermotectonic evolution of the North Pyrenean Agly Massif during Early Cretaceous hyperextension using multi-mineral U-Pb thermochronometry. *Tectonics*, 38, 1509–1531.

Péron-Pinvidic, G., Manatschal, G., Minshull, T. A., and Sawyer, D. S. (2007). Tectono sedimentary evolution of the deep Iberia-Newfoundland margins: Evidence for a complex breakup history. *Tectonics*, 26, 1–19.

Peybernès, B. (1976). *Le Jurassique et le Crétacé inférieur des Pyrénées franco-espagnoles entre la Garonne et la Méditerranée*. Thèse sci. nat., Université de Toulouse.

Pope, R., Wilkinson, K., Skourtsos, E., Triantaphyllou, M., and Ferrier, G. (2008). Clarifying stages of alluvial fan evolution along the Sfakian piedmont, southern Crete: new evidence from analysis of post-incisive soils and OSL dating. *Geomorphology*, 94, 206–225.

Pope, R. J., Candy, I., and Skourtsos, E. (2016). A chronology of alluvial fan response to Late Quater-

nary sea level and climate change. *Crete Quaternary Res.*, 86, 170–183.

Rahl, J., Fassoulas, C., and Brandon, M. (2004). Exhumation of high-pressure metamorphic rocks within an active convergent margin, Crete, Greece: a field guide. In Guerrieri, L., Rischia, I., and Serva, L., editors, *Field Trip Guidebook for the 32nd International Geological Congress*, pages 1–36. Italian Agency for the Environmental Protection and Technical Services, Rome.

Rahl, J. M., Anderson, K. M., Brandon, M., and Fassoulas, C. (2005). Raman spectroscopic carbonaceous material thermometry of low-grade metamorphic rocks-calibration and application to tectonic exhumation in Crete, Greece. *Earth Planet. Sci. Lett.*, 240, 339–354.

Rape, A. (1960). Recent development of mountain slopes in Karkevagge and surroundings, northern Scandinavia. *Geogr. Ann.*, 42, 73–200.

Reneau., S., Dietrich, W. E., Donahue, D. J., Jull, A. J. T., and Rubin, M. (1990). Late Quaternary history of colluvial deposition and erosion in hollows, central California Coastal Ranges. *Geol. Soc. Am. Bull.*, 102, 969–982.

Sanders, D. (2010). Sedimentary facies and progradational style of a Pleistocene talus-slope succession, Northern Calcareous Alps, Austria. *Sediment. Geol.*, 228, 271–283.

Sanders, D., Ostermann, M., and Kramers, J. (2009). Quaternary carbonate-rocky talus slope successions (Eastern Alps, Austria): sedimentary facies and facies architecture. *Facies*, 55, 345–373.

Seidel, M. (2003). *Tectono-sedimentary evolution of middle Miocene supra-detachment basins (western Crete, Greece)*. PhD thesis, University of Köln. 116 p.

Sharpe, C. F. S. (1938). *Landslides and Related Phenomena*. Columbia University Press, New York.

Shukla, M. K. and Sharma, A. (2018). A brief review on breccia: it's contrasting origin and diagnostic signatures. *Solid Earth Sci.*, 3(2), 50–59.

Sibuet, J. C., Srivastava, S. P., and Spakman, W. (2004). Pyrenean orogeny and plate kinematics. *J. Geophys. Res.*, 109, article no. B08104.

Skourtsos, E., Pope, R. J. J., and Triantaphyllou, M. (2007). Tectono-sedimentary evolution and rates of tectonic uplift of the Sphakia coastal zone, southwest Crete. *Bull. Geol. Soc. Greece*, XXXVII, article no. 475e487.

Souquet, P. and Debroas, E. (1980). Tectorogenèse

et évolution des bassins de sédimentation des Pyrénées pendant le cycle alpin. In *Évolutions géologiques de la France*, volume 107 of *26e congr. géol. int., colloque C7. Mém*, pages 213–233. BRGM, Orléans.

Theye, T., Seidel, E., and Vidal, O. (1992). Carpholite, sudoite, andchloritoid in low-grade high-pressure metapelites from Creteand the Peloponnese, Greece. *Eur. J. Mineral.*, 4, 487–507.

Thomson, S. N., Stöckhert, B., and Brix, M. R. (1998). Thermochronology of the high-pressure metamorphic rocks of Crete, Greece: implications for the speed of tectonic processes. *Geology*, 26, 259–262.

Thomson, S. N., Stöckhert, B., and Brix, M. R. (1999). Micocene high-pressure metamorphic rocks of Crete, Greece: rapid exhumation by buoyant escape. In Ring, U., Brandon, M. T., Lister, G. S., and Willet, S. D., editors, *Exhumation Processes: Normal Faulting, Ductile Flow and Erosion*, volume 154 of *Special Publications*, pages 87–108. Geological Society, London.

Tsimi, C., Ganas, A., Ferrier, G., Drakatos, G., Pope, R. J., and Fassoulas, C. (2007). Morphotectonics of the Sfakia normal fault, southwestern Crete, Greece. In *Proceedings of 8th Pan-Hellenic Geographical Conference, Athens, Greece, 2007 October 4–7*, pages 186–194.

Varnes, D. J. (1978). Slope movement types and processes. In Schuster, R. L. and Krizek, R. J., editors, *Landslides, Analysis and Control, Special Report 176: Transportation Research Board*, pages 11–33. National Academy of Sciences, Washington, DC.

Vaudin, J. L. (1982). *Etude géologique de la couverture mésozoïque du massif de l'Agly (entre Estagel et Baixas, Pyrénées-Orientales)*. Thèse 3e cycle, Université de Toulouse 3. 157 p.

Vidakis, M., Triantaphyllis, M., and Mylonakis, I. (1993). *Geological map of Greece (1/50,000), Vrisses sheet*. The Institute of Geology and Mineral Exploration of Greece (IGME), Athens.

Zambetakis-Lekkas, A., Pomoni-Papaioannou, F., and Alexopoulos, A. (1998). Biostratigraphical and sedimentological study of Upper Senonian–Lower Eocene sediments of Tripolitza Platform in central Crete (Greece). *Cretac. Res.*, 19, 715–732.